

**CHAPTER 5**  
**PHENOTYPIC AND MOLECULAR**  
**EXAMINATION OF A HYPER-MOTILE**  
***ACINETOBACTER BAUMANNII* VARIANT**  
**STRAIN**

## 5.1 Introduction

Long-term survival of *A. baumannii* in the hospital environment can be attributed to a high level of environmental resilience. This enables enhanced opportunities for transmission between patients either via human reservoirs or inanimate materials (Section 1.2.2.1). Adherence and motility are important factors that can influence the ability of organisms to effectively colonise surfaces and subsequently form biofilms (Sections 1.2.4 and 1.2.2.2).

Adherence, in the form of biofilms, is critical for colonisation of medical equipment, making the cleaning and decontamination of these devices extremely difficult and often ineffectual. As such, biofilms represent a major source of *A. baumannii* cross-contamination in the hospital setting (Dijkshoorn *et al.* 2007). The biofilm mode of life also provides a remarkable resilience to the organism during infection as their often tight and complex structures effectively shield bacteria from antibiotics or host defence mechanisms (Hoiby *et al.* 2010). Consequently, biofilms formed in various parts of the human body as a result of disease are regarded as major obstacles limiting the effectiveness of antibiotic treatments. Not only do biofilms often result in an increased level of resistance, many bacteria, including *A. baumannii*, have the ability to increase biofilm formation upon exposure to sub-inhibitory concentrations of antimicrobial compounds (Nucleo *et al.* 2009). Multicellular biofilm populations under continuous stress, such as *P. aeruginosa* in a chronic cystic fibrosis infection, have also been linked to increased genetic variation, possibly by the uptake of DNA found within the biofilm (Oliver *et al.* 2000). Moreover, a higher than normal mutation rate of a bacterial species in a population may contribute to the success of the pathogen in the host environment by for example altering surface structures in order to circumvent the host immune response (Hoboth *et al.* 2009; Livorsi *et al.* 2011; Seifert 1996). Conversely, progenies expressing a higher virulence potential may also be generated by hypermutable strains (Naughton *et al.* 2011).

Whereas various molecular mechanisms involved in adherence of *A. baumannii* to abiotic surfaces have been identified (Choi *et al.* 2009; Loehfelm *et al.* 2008; Tomaras *et al.* 2003), little is known about the molecular mechanisms involved in *A. baumannii* motility. In this study, a hyper-motile variant of strain ATCC 17978 was isolated, and characterisation of this variant by means of phenotypic, genetic and

transcriptomic analyses assisted in identification of various novel molecular mechanisms that may play a role in motility and adherence characteristics of *A. baumannii*. Furthermore, the effect of environmental stress, such as low-iron conditions, high salinity or antibiotic pressure, on motility and adherence was examined.

## 5.2 Results and Discussion

### 5.2.1 Isolation of *A. baumannii* 17978hm; a hyper-motile variant strain

#### 5.2.1.1 Motility characteristics

Motility of *A. baumannii* ATCC 17978 is evident only on LB media containing <0.5% agar (Section 2.3.4). However, colonies with a distinct morphology on LB medium containing 1% agar were identified in a culture streaked from a cryopreserved ATCC 17978 stock. The colony edge displayed a minor, though noticeable, motile appearance (Figure 5.1). This phenotype could be further enhanced when the isolated variant and ATCC 17978 cells were cultured on semi-solid MH media. Unlike WT ATCC 17978 cells, the variant displayed a motile phenotype on MH containing 0.25% agar which was similar to that observed on semi-solid LB media. The multiple colonies displaying this distinct motile morphology that were isolated from the cryopreserved stock all showed the same phenotype on semi-solid LB and MH media. These variants were designated hyper-motile and subsequently one representative was further investigated.

A number of analyses were carried out to confirm that the hyper-motile variant was a derivative of *A. baumannii* strain ATCC 17978. First, the hyper-motile variant strain was demonstrated to have the ability to grow at 44°C, a characteristic commonly used for identification of *A. baumannii* (Bouvet and Grimont 1987). Examination using bright-field microscopy revealed no morphological differences between WT and variant cells (data not shown). Furthermore, the growth rates of the two strains appeared similar in MH broth (Figure 5.2) and resistance levels to various different antimicrobials were indifferent (Section 5.2.8.1; Table 5.4). To analyse the protein content of the WT and variant strains, cells from each strain were harvested from semi-solid MH media, disrupted and centrifuged twice at different centrifugal forces in order to separate the cytosolic and membrane fractions of the cells (Section 2.6.1). The protein content of the cytosolic and membrane fractions of the WT and hyper-motile cells were compared by electrophoresis of approximately 60 µg total

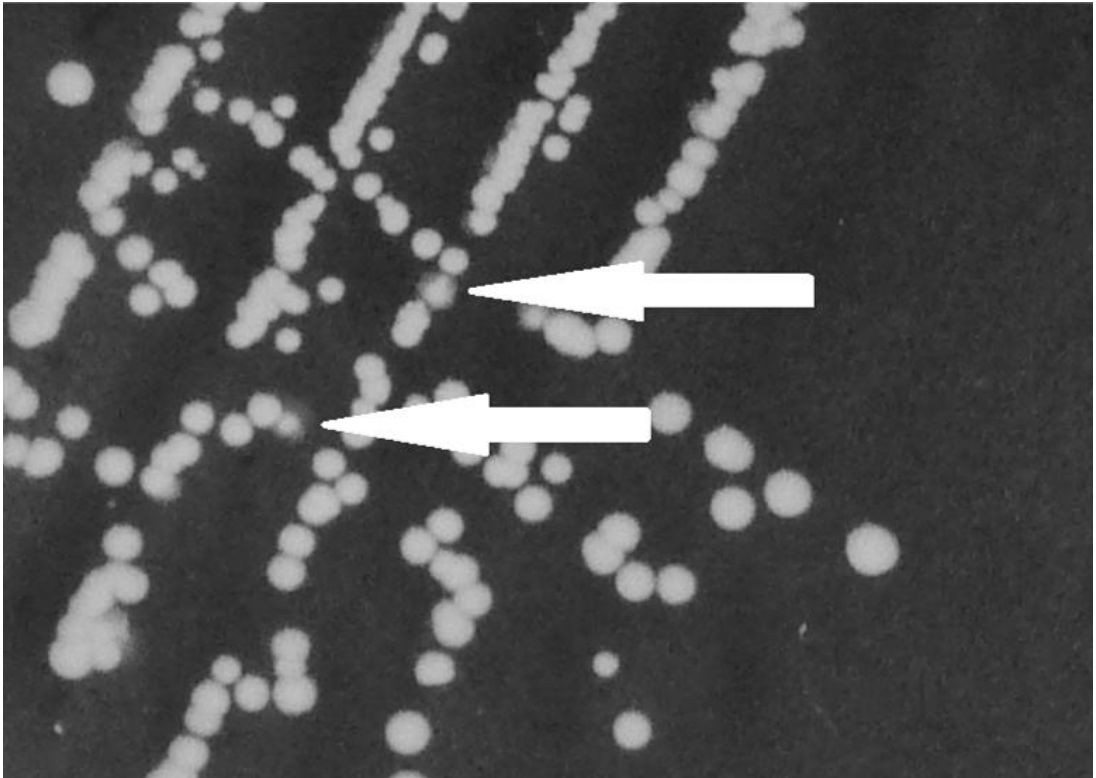


**Figure 5.1: Identification of the hyper-motile variant strain**

Colonies with a distinct morphology (indicated by the white arrows) were identified in an *A. baumannii* ATCC 17978 culture streaked from a cryopreserved (-80°C) stock. WT colonies are round and possess a dense edge on LB medium containing 1% agar. The colonies formed by the variant display a diffuse edge on this solid medium.

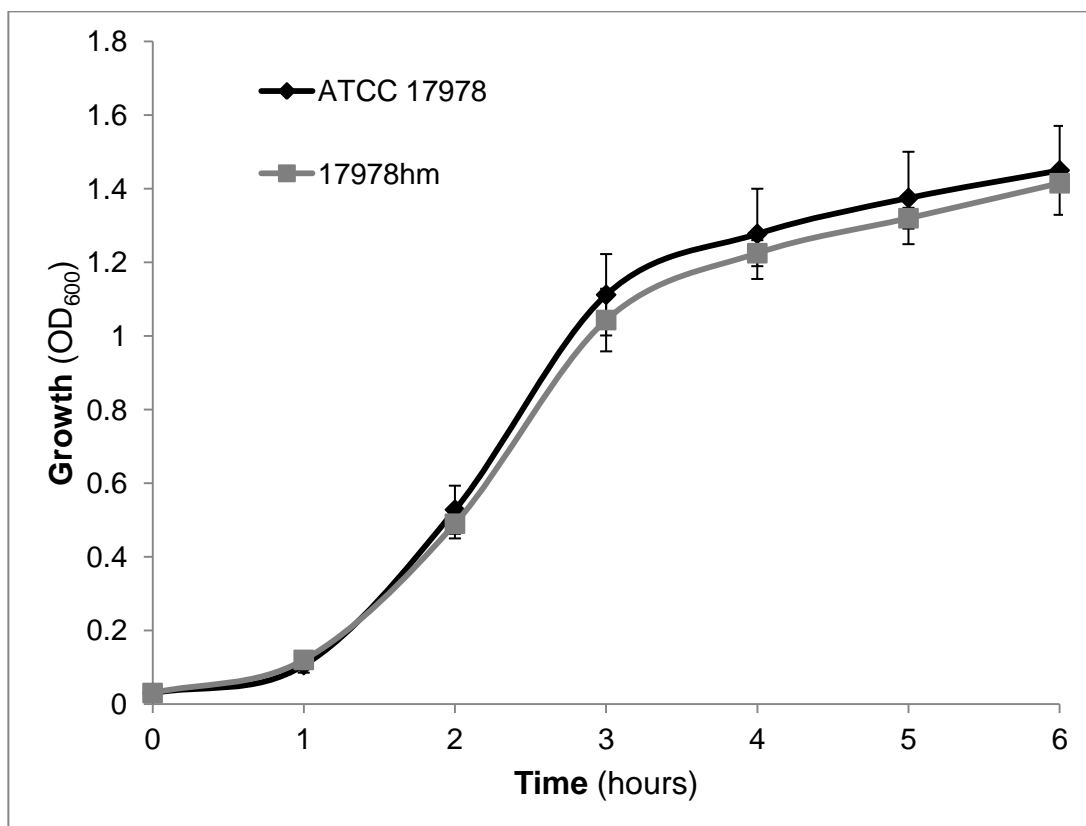


**Figure 5.2: Growth curves of *A. baumannii* ATCC 17978 and the hyper-motile variant**

The growth rate of *A. baumannii* ATCC 17978 and the hyper-motile variant (*A. baumannii* strain 17978hm) was investigated in MH broth. ON cultures were diluted 1:50 into fresh MH broth and the OD<sub>600</sub> was measured hourly, up to 6 hours. The experiments were performed three times on different days. The error bars represent the standard deviation. Significant differences were not observed between the growth rate of strains ATCC 17978 and 17978hm.

protein on a 12% SDS-polyacrylamide gel (Section 2.6). Although phenotypically distinct, the Coomassie stained protein profile (Section 2.6.4) revealed no major differences between the two isolates (Figure 5.3).

PCR analysis using oligonucleotides specific for detection of a gene encoding a transporter protein (A1S\_2562; Table 2.4) was positive in both strains. This minimised the possibility of contamination by other *A. baumannii* isolates used in this study, as A1S\_2562 was only detected in strain ATCC 17978 and not in any of the other *A. baumannii* isolates in the laboratory collection (Table 6.1). Detection of the A1S\_2562 gene and other analyses, including protein content comparison, growth rate and resistance indicated that the variant obtained was a derivative of strain ATCC 17978. The hyper-motile isolate is subsequently referred to as *A. baumannii* 17978hm.

#### **5.2.1.2 Stability of the variant strain**

Motility mechanisms are unlikely to be required when culturing takes place in broth and it is possible that this phenotype could be lost upon sequential sub-culturing. Therefore, the 17978hm phenotype was investigated after sub-culturing in MH broth, once daily (1:100), for a total duration of 5 days. The 17978hm variant appeared stable, as the colony morphology was similar between one-day and five-days old cultures plated onto solid LB agars (data not shown). The WT *A. baumannii* ATCC 17978 cells were also investigated for their ability to switch to a hyper-motile phenotype. Therefore, three colonies were individually resuspended in 1 ml LB broth, diluted (1:1000) and spread plated for single colonies on LB media containing 1% agar. The morphology of approximately 5000 colonies per replicate was examined for possible variations, however, no motile colonies (as seen in Figure 5.1) were identified. WT colonies were also spotted onto MH media containing 0.25% agar, this would allow cells to translocate across the medium if they switched to a hyper-motile state. However, growth was only observed at the inoculation site (data not shown). In order to investigate a potential influence of cryopreservation in promoting hyper-motility, the same experiments, e.g. spread-plating on solid LB and spotting on semi-solid MH, were performed with isolated WT cells that underwent the same storage conditions as the original stock containing the variant strain. However, no switching to hyper-motility was observed after storage at -80°C for more than one week (data not shown). These experiments indicated that the switch to

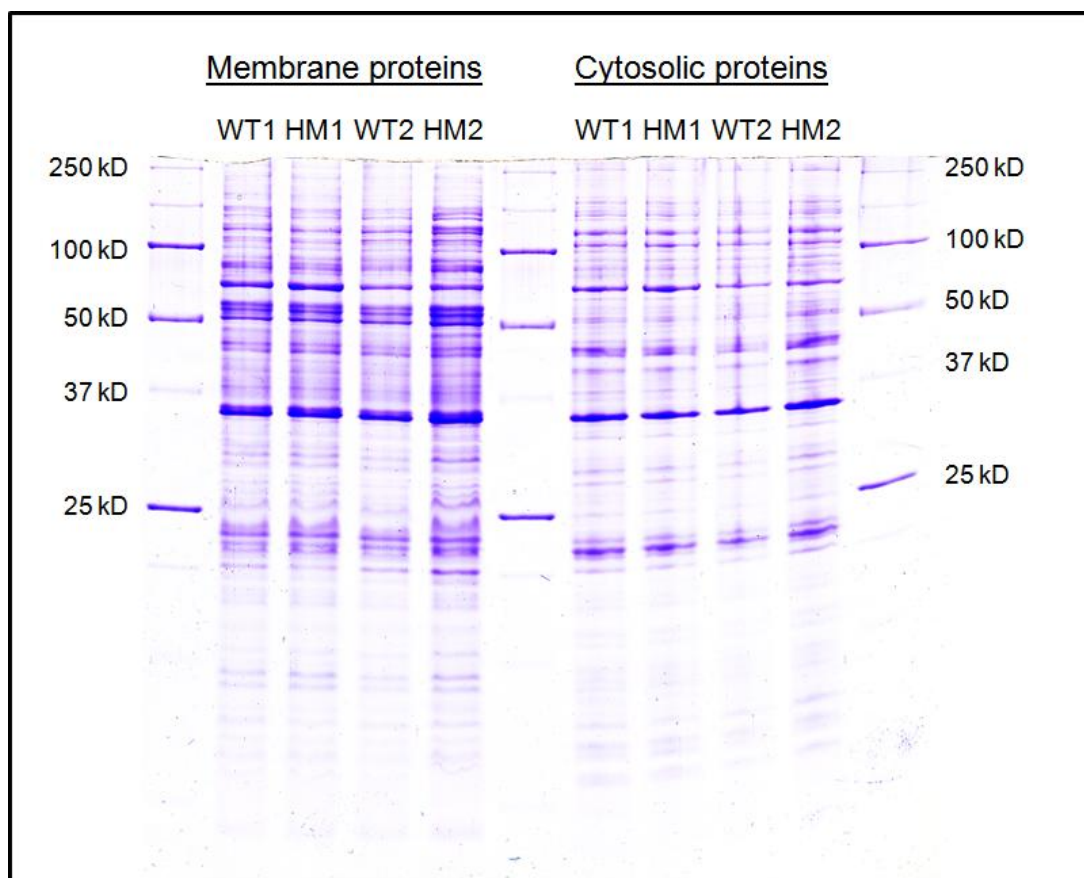


**Figure 5.3: Analysis of the protein content of *A. baumannii* strain ATCC 17978 and the hyper-motile variant**

The protein content of two replicates of *A. baumannii* strain ATCC 17978 (WT1 and WT2) and the hyper-motile variant (HM1 and HM2) were compared by SDS-PAGE (12%) and visualised by Coomassie staining (Section 2.6). The cytosolic and membrane fractions of the cells were isolated by cell fragmentation followed by a two-step centrifugation process (Section 2.6.1). No significant differences were observed in the duplicate comparative analysis of either the cytosolic or membrane associated proteins. The precision Plus Dual Color protein markers (Bio-Rad) was run in triplicate for referencing purposes, the molecular weights have been provided on both sides of the gel.

the hyper-motile phenotype occurred in less than 1 in 5000 cells. Overall, the WT and hyper-motile variant were sufficiently stable for further characterisation.

## **5.2.2 Adherence characteristics**

### **5.2.2.1 Adherence to abiotic surfaces and biofilm formation**

Biofilm formation is a complex process initiated by attachment to a surface, followed by the creation of a multilayered biomass containing secondary structures. The ability of strain 17978hm to adhere to abiotic surfaces may differ to that of WT cells as surface structures and/or secretins could be involved in the altered motility phenotype. Nevertheless, examination of abiotic surface adherence using a static biofilm assay (Section 2.3.3) revealed no significant differences between WT and 17978hm cells (Figure 5.14). However, this may be due to limitations of the microtiter tray biofilm formation assay used in this study. After staining, but before washing, wells containing strain 17978hm showed a noticeable increase in biomass compared to that of wells containing WT cells (data not shown). This difference was not seen after washing, indicating that strain 17978hm forms cell aggregates that are only loosely attached to the surface of the microtiter tray. Furthermore, the WT strain did not produce large amounts of biofilm and the adhering cells appeared to form a monolayer only (Section 4.2.3). Of note, the assay as described in Section 2.3.3 was modified by increasing the volume (from 150 to 200  $\mu$ l) of the solutions during staining, washing and release of the dye. Thus, cells that adhered to the polystyrene at the air-liquid interface, or meniscus, were also investigated. Consequently, the levels of biofilm formed by strain ATCC 17978 described here were higher compared to those observed in Section 4.2.3.

### **5.2.2.2 Pellicle formation**

Pellicle formation may play an important role in environmental persistence of *A. baumannii* (Section 1.2.2). Although little is known about the mechanisms responsible for intercellular interactions in *A. baumannii* pellicles, the differences between the WT and 17978hm may lead to changes in this phenotype. To investigate pellicle formation, WT and 17978hm cultures were incubated for 72 hours in polypropylene tubes with a 1.4 cm diameter without shaking. The pellicle was isolated using methanol dehydration, transferred to a clean 1.5 ml tube and the dry weight was subsequently determined on an analytical balance (Section 2.3.5). Various different temperatures and media were tested using both *A. baumannii* strain ATCC 17978 and 17978hm. Firstly, pellicle formation by *A. baumannii* strains

ATCC 17978 and 17978hm was only observed at 25°C and not at 37°C (data not shown), which correlates with similar studies (Marti *et al.* 2011). Both strain ATCC 17978 and 17978hm were found to not form pellicles in MH media and pellicle formation levels fluctuated in LB media (data not shown). Consistently high levels were observed in strain 17978hm when incubated for 72 hours at 25°C using LB media with lower salt concentrations, these being 100 mM NaCl instead of approximately 171 mM NaCl (1%) which was used in standard LB media; the WT strain was unable to form pellicles under these conditions (Figure 5.4). Measurement of planktonic growth of strain 17978hm was significantly lower than that of strain ATCC 17978 in the pellicle assays,  $OD_{600} = \sim 0.15$  and  $\sim 0.50$ , respectively. This may be due to reduced oxygen levels in the growth medium as a result of the high oxygen dependency of the pellicle itself (Liang *et al.* 2010). Hence, oxygen tension in the growth medium of strain 17978hm would have been lowered resulting in reduced levels of planktonic growth. Intercellular connections in a pellicle require molecular complexes of proteins, DNA or exopolysaccharides (Coulon *et al.* 2010; Liang *et al.* 2010). Performing the pellicle formation assays with strain 17978hm in LB media with reduced salt concentration supplemented with varying concentrations of DNase I (100, 500, 1000 or 5000 U/ml) or proteinase K (100 or 500 µg/ml) did not result in a significant alteration of pellicle biomass (data not shown). Additionally, examination of pellicle structures transferred to a glass slide and subsequently treated with either DNase I or proteinase K using the concentration stated above had no effect on the integrity of the pellicle structure (data not shown). This indicated that neither DNA, nor extracellular protein structures were essential for pellicle formation or pellicle stability in *A. baumannii* 17978hm.

### 5.2.2.3 Adherence to eukaryotic cells

Adherence to abiotic and biotic surfaces appears to be mediated by different molecular mechanisms in most *A. baumannii* strains (Sections 1.2.3 and 4.2). Therefore, despite the similar levels observed in abiotic surface adherence (Section 5.2.2.1), adherence to biotic surfaces by strains ATCC 17978 and 17978hm was investigated (Section 2.3.6). In order to emphasise potential differences between WT and 17978hm cells, bacterial cells for inoculum preparation were harvested from semi-solid MH media, on which only strain 17978hm displayed a motile state. After incubating the bacteria ( $\sim 1 \times 10^7$  CFU) in conjunction with the eukaryotic cells for 4

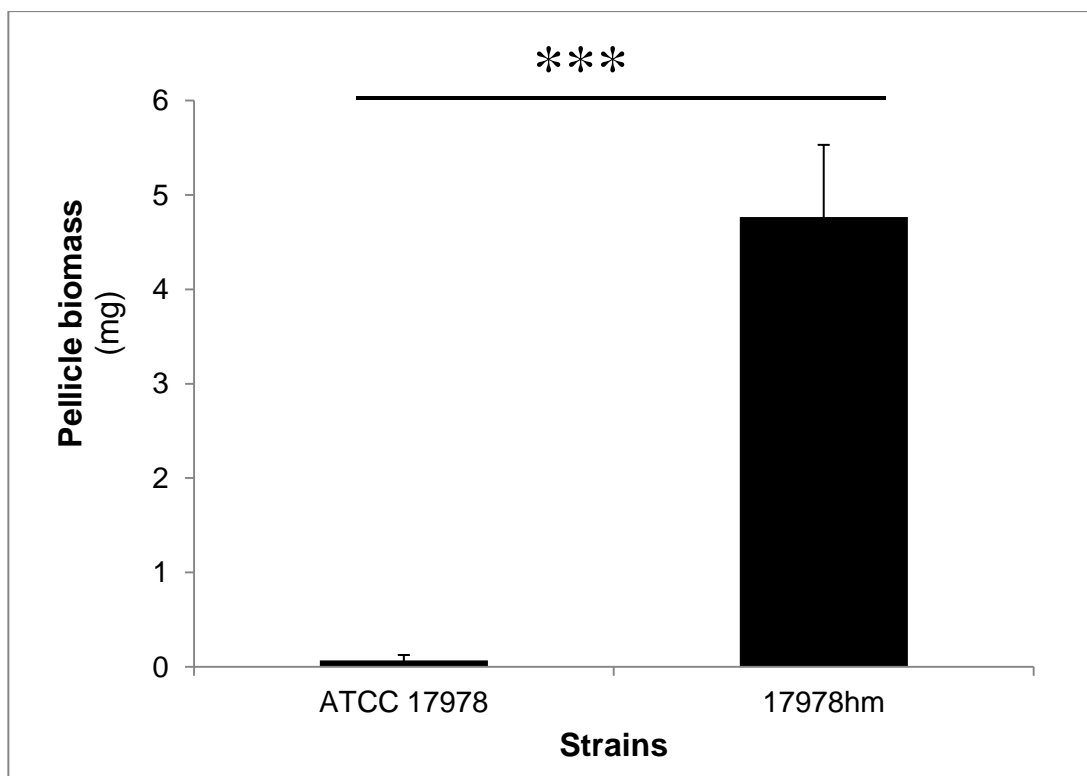


**Figure 5.4: Pellicle formation by *A. baumannii* strains ATCC 17978 and 17978hm**

The pellicles of *A. baumannii* strains ATCC 17978 and 17978hm were examined after incubation for 72 hours at 25°C in polypropylene tubes with a diameter of 1.4 cm (Section 2.3.5). The film of cells that formed the pellicle was isolated using methanol. The biomass in milligram (mg) was measured after centrifugation and dehydration. A significant difference ( $p < 0.001$ ) between the two strains was observed using a two-tailed student *t*-test and is indicated by the asterisks. Experiments were performed at least three times, the error bars represent the standard deviation.

hours, the number of 17978hm cells that were recovered from washed A549 pneumocytes was significantly higher than the number of ATCC 17978 cells (1.7-fold;  $p < 0.05$ ) (Figure 5.5). These elevated levels were not a result of an increased growth rate in the cell culture medium (data not shown). This difference revealed that there is no direct correlation between binding to abiotic and biotic surfaces. However more importantly, the hyper-motile variant strain may exhibit a higher disease potential as a result of an increased ability to adhere to cells of the human respiratory tract. Noteworthy, this assay does not differentiate between bacterial cells adhering to the eukaryotic cell surface and those invading and potentially replicating intracellularly.

### 5.2.3 Cell surface hydrophobicity

The differences between the phenotypes of the WT and 17978hm *A. baumannii* cells described above may be related to cell surface properties. Therefore, the hydrophobicity of the cells was investigated using the microbial adhesion to hydrocarbons (MATH) test (Section 2.3.7) (Rosenberg *et al.* 1980). Four *A. baumannii* strains were included in the analysis; ATCC 19606 as a hydrophilic control (McQueary and Actis 2011), ACICU as a hydrophobic control (identified in preliminary assays, data not shown), and ATCC 17978 and 17978hm. ON cultures of these strains were diluted (1:10) and grown for 2 hours. The cells were then washed twice using PUM buffer (Table 2.1), the OD<sub>600</sub> was adjusted to 0.25 in the same buffer and these cell suspensions were incubated for 20 minutes at 30°C. Xylene was added to the solution and mixed thoroughly with the aqueous phase. The two phases were allowed to separate and the optical density of the aqueous phase was subsequently measured. The OD<sub>600</sub> values obtained before and after mixing with xylene were used to calculate the hydrophobicity index (Section 2.3.7). The majority of ATCC 19606 cells were found to be retained in the aqueous phase confirming their hydrophilic properties (Figure 5.6). Conversely, nearly all the ACICU cells bound to xylene resulting in an almost complete loss of cells in the aqueous phase. A significant increase in hydrophobicity of 17978hm cells (HI = 40%) compared to WT cells (HI = 17%) was observed using a two-tailed student *t*-test ( $p < 0.05$ ). It is tempting to speculate that this increased hydrophobicity may be linked to enhanced motility and adherence. However, in eight distinct clinical *A. baumannii* isolates studied recently, the degree of hydrophobicity could not be linked directly

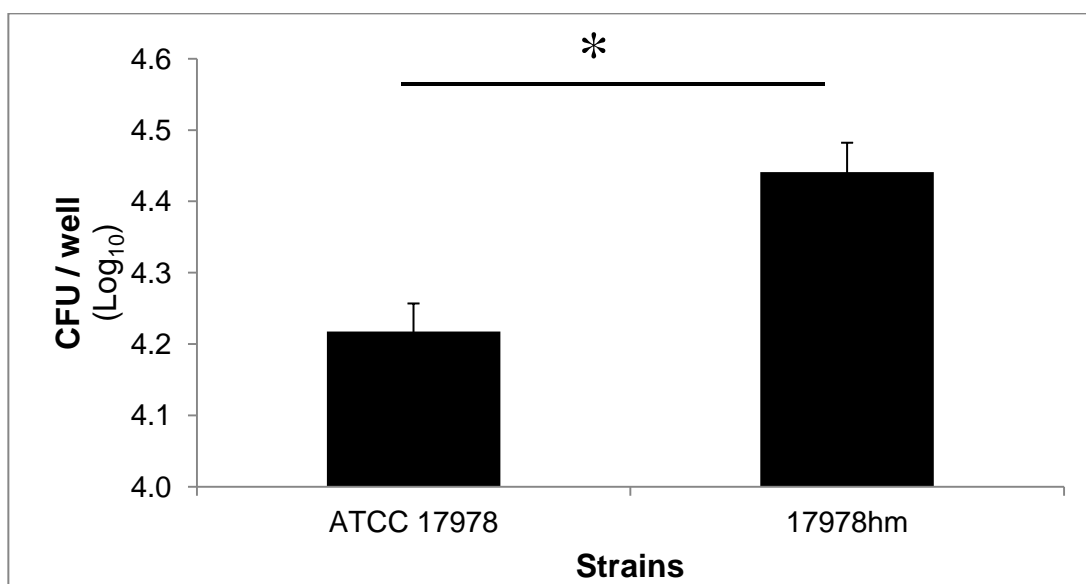


**Figure 5.5: Adherence to A549 human lung epithelial cells**

The number of colony forming units (CFUs) in Log<sub>10</sub> values of *A. baumannii* ATCC 17978 and 17978hm that were recovered from a washed A549 cell culture after incubation for 4 hours are shown (Section 2.3.6). A significant difference ( $p < 0.05$ ) between the two strains was observed using a two-tailed student *t*-test and is indicated by the asterisk. Error bars show the standard error of the mean.

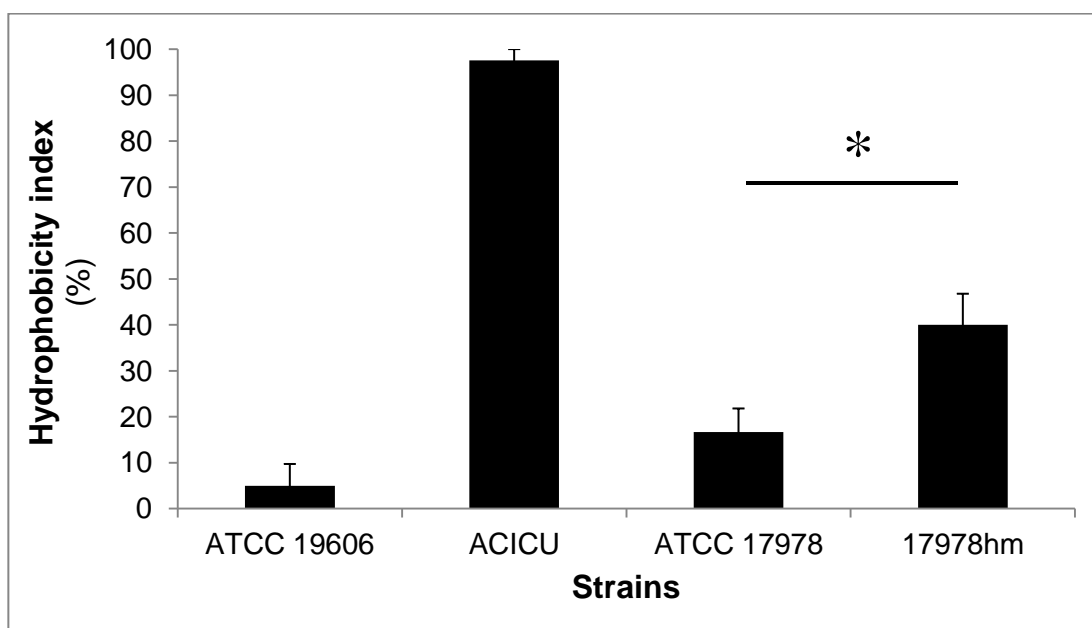


**Figure 5.6: Cell surface hydrophobicity**

The hydrophobicity index of *Acinetobacter* cells was calculated by measuring the cell density of the aqueous phase before and after mixing with xylene (Section 2.3.7). Strain ATCC 19606 represents a hydrophilic control (McQueary and Actis 2011) and strain ACICU possesses hydrophobic properties. A significant increase in hydrophobicity was determined in strain 17978hm compared to strain ATCC 17978 ( $p < 0.05$ ; two-tailed student *t*-test) and is indicated by the asterisk. The data represent results obtained on three separate days and the error bars show the standard deviation.

to either motility or adherence characteristics (McQueary and Actis 2011). Nevertheless, a correlation between biofilm formation and hydrophobic characteristics was shown in two other studies (Costa *et al.* 2006; Pour *et al.* 2011). Interestingly, the hydrophobic isolates did not possess an increased ability to adhere to biotic surfaces (Costa *et al.* 2006). Therefore, the role of increased hydrophobicity in the phenotypic alterations observed in 17978hm cells requires further investigation (Section 7.2.2).

## **5.2.4 Transcriptomic analysis of the motile versus non-motile population**

### **5.2.4.1 Design of the study**

Comparative analysis of the proteome or transcriptome of cells in distinct life styles may provide information about the molecular mechanisms and regulatory pathways responsible for driving a population into a certain mode of living. Furthermore, other ‘secondary’ mechanisms differentially represented may be identified; these are often not considered when taking a more specific experimental approach, such as qRT-PCR. *A. baumannii* strains 17978hm and ATCC 17978 were grown on semi-solid MH media in order to distinguish between motile and non-motile populations, respectively. Approximately eight hours of growth was required to yield a sufficient number of motile 17978hm cells for transcriptomic analysis. The cells were collected using pre-chilled PBS and resuspended after centrifugation in TRIzol<sup>®</sup> reagent (Invitrogen, Australia) (Section 2.4.3). The RNA was extracted from the aqueous phase using the PureLink<sup>™</sup> Micro-to-Midi Total RNA Purification kit (Invitrogen). The integrity of the total RNA was assessed by gel electrophoresis (Section 2.4.4) and by measuring both the OD<sub>260</sub>/OD<sub>280</sub> and the OD<sub>260</sub>/OD<sub>230</sub> values, to ensure minimal contamination by protein and salt/detergents, respectively (Section 2.4.6). The cDNA synthesis and labelling using the Agilent Fairplay Microarray Labelling Kit (Stratagene) was performed by the Ramaciotti Centre for Gene Function Analysis, University of New South Wales, Australia (Section 2.5.2). The Ramaciotti Centre also performed the hybridisation of the labelled cDNA to the microarray containing probes for all predicted ORFs of the ATCC 17978 genome (Sections 2.5.1 and 2.5.2). The same microarray was used to investigate the transcriptomic responses of *A. baumannii* ATCC 17978 to iron limitation (Section 3.2.2). The statistical analysis of the transcriptomic differences between WT and 17978hm cells was performed with SAM (Tusher *et al.* 2001).

#### 5.2.4.2 *Global transcriptional differences between motile and non-motile cells*

Major transcriptional differences were observed between the motile and non-motile populations (Figure 5.7). More than 2-fold differential expression was observed for 576 genes, of which 348 (10.3%) genes were down-regulated and 228 (6.8%) up-regulated (Appendices D and E). During the course of this study, genes differentially expressed more than 4-fold ( $\text{Log}_2=2$ ) were the predominant point of focus, this included 90 down-regulated genes and 61 up-regulated genes. Various genes functioning in metabolism were found to be down-regulated in the motile population, such as those encoding members of the phenylacetic acid degradation pathway. Down-regulation of metabolic pathways was also observed in transcriptional investigation of swarming *P. aeruginosa* cells (Tremblay and Deziel 2010). The microarray results were linked to the COG-function classes to investigate changes within certain functional groups (Figure 5.8). The four genes of an up-regulated type I pili cluster (A1S\_1507-1510; Figure 5.7) accounted for the approximately 9% up-regulated genes assigned to the motility COG. There is no previous evidence for a role of type I pili in promotion of surface translocation, in contrast, motility rates appeared to be repressed by type I pili in *X. fastidiosa* (De La Fuente *et al.* 2007). However, other phenotypes, such as increased adherence to human epithelial cells, may be associated with overexpressed type I pili in strain 17978hm.

A gene cluster predicted to encode a type VI secretion system (A1S\_1292-1311) was found to be up-regulated in the motile population. Type VI secretion systems may contribute to bacterial pathogenicity (Mougous *et al.* 2006), indicating that the motile cells could possess a greater virulence potential compared to non-motile cells. However, the gene cluster coding for the type VI secretion system can also be found in the non-pathogenic *A. baumannii* strain SDF. Mauve analysis (Section 2.7.2) also showed that four ORFs encoding proteins of unknown function have replaced the type VI secretion system gene cluster in the community-acquired *A. baumannii* strain D1279779 (data not shown). The type VI secretion system may also be non-functional in strain 1656-2, a strain capable of forming well developed biofilms (Shin *et al.* 2009), as it contains an insertion element in A1S\_1302 (data not shown). Therefore, the function of the type VI secretion system in *A. baumannii* requires further investigation (Section 7.1). In *E. coli*, the type VI secretion system appears to play a role not only in eukaryotic cell adherence and pathogenesis, but also in

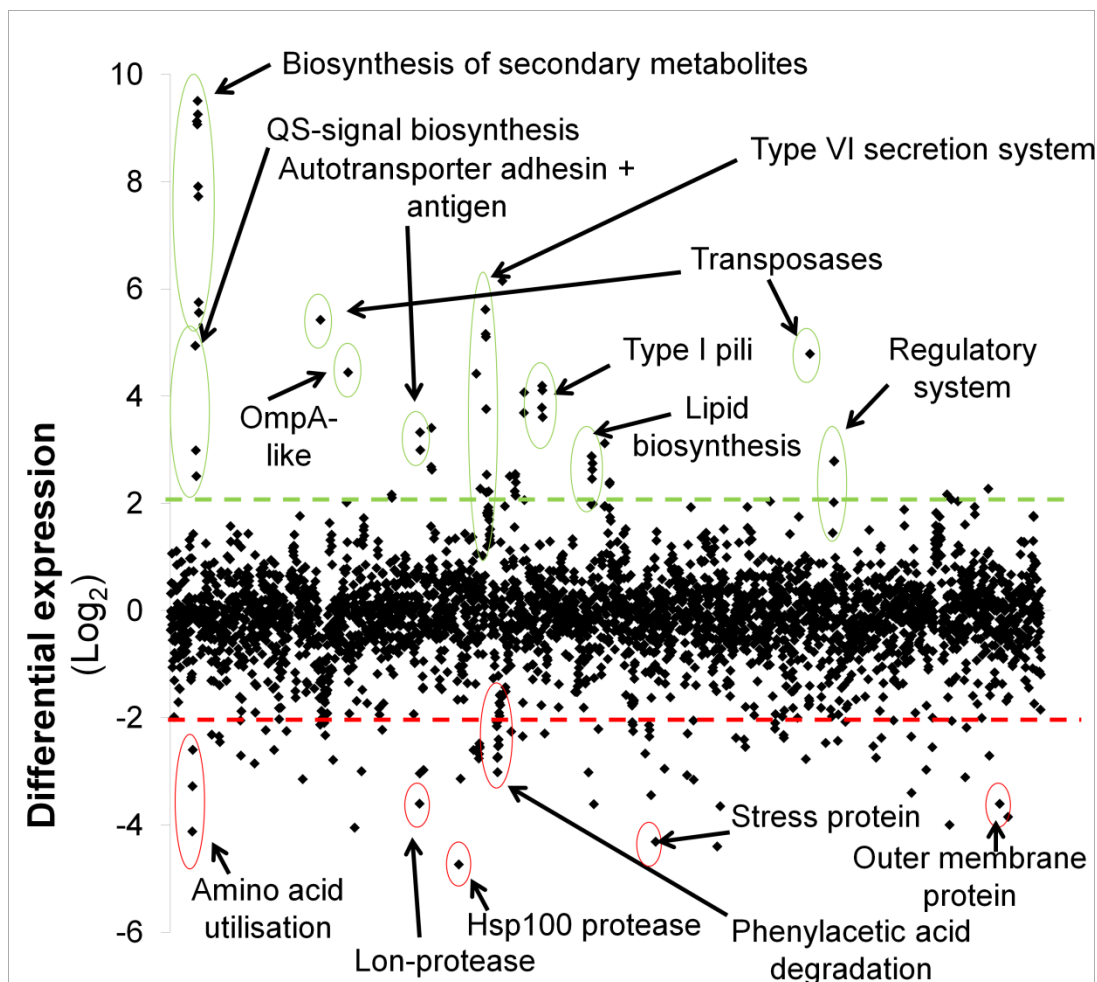


**Figure 5.7: Overview of transcriptional differences between motile and non-motile *A. baumannii* cells**

The microarray results have been displayed as the differential expression of the motile versus the non-motile population in  $\text{Log}_2$ -values (Section 2.5). The diamond markers indicate the differential expression levels of all predicted ORFs of the ATCC 17978 genome and are sorted on the X-axis according to the locus-tag. The dashed lines indicate 4-fold ( $\text{Log}_2=2$ ) differential expression, up-regulated genes in the motile populations are located above the green line and down-regulated genes below the red line. Examples of differentially expressed genes are indicated in the figure, such as the genes involved in biosynthesis of quorum-sensing (QS) signals and Lon protease. The lists of genes differentially expressed by more than 2-fold can be found in Appendices D and E.

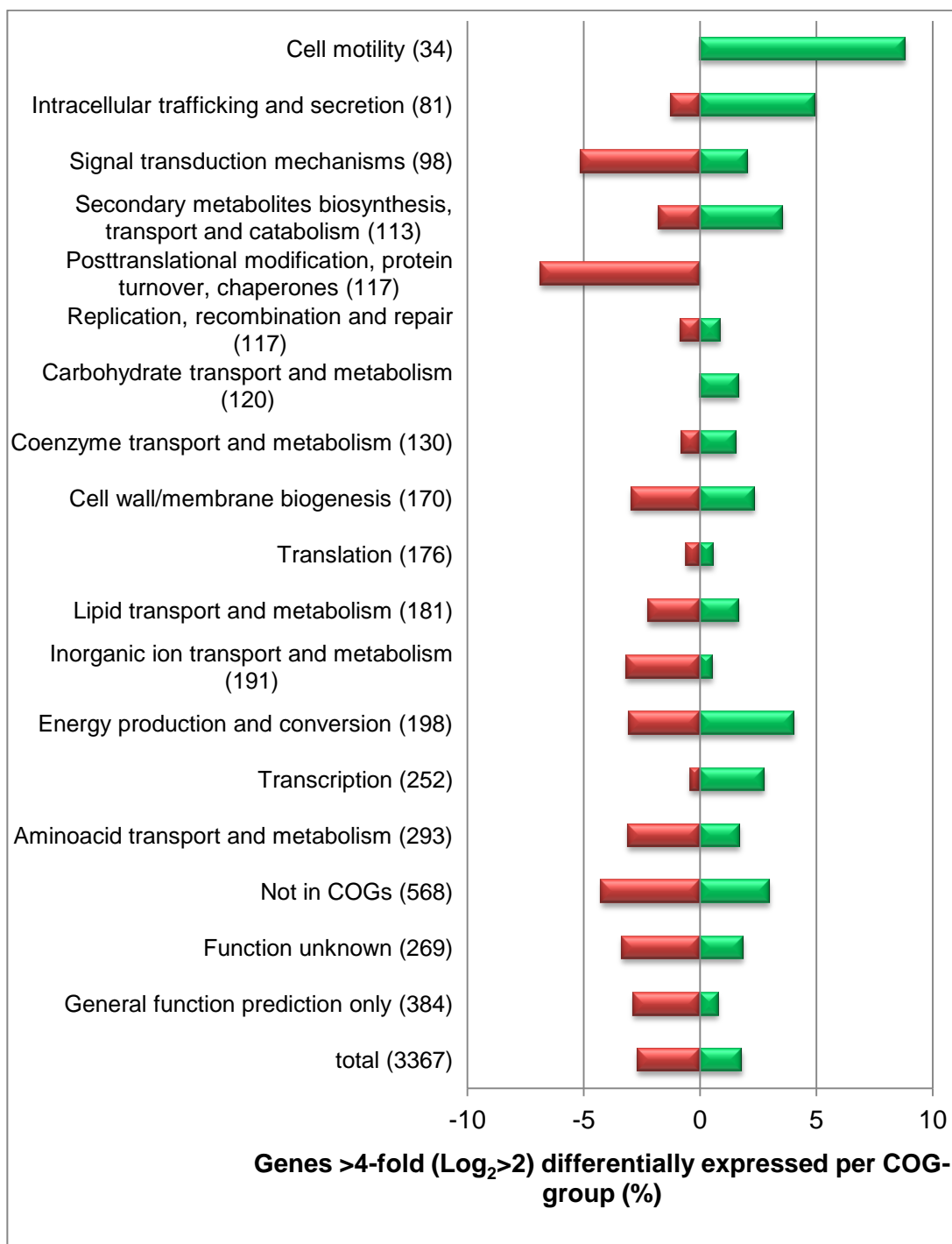


**Figure 5.8: Transcriptomic data of motile versus non-motile *A. baumannii* cells represented by COG function**

Depiction of the clustering of orthologous groups (COG) and the percentage of up-regulated (green) and down-regulated (red) genes within such group as determined by microarray analysis. Genes differentially expressed >4-fold ( $\text{Log}_2 > 2$ ) were included only for preparation of this figure. The total number of genes per COG is shown in parentheses.

regulation of type I pili expression (de Pace *et al.* 2010), potentially explaining the up-regulation of A1S\_1507-1510.

Another factor that has a potential to increase the adherence and virulence characteristics of strain 17978hm as compared to ATCC 17978 cells is an autotransporter adhesin and a putative antigen encoded by the overexpressed genes A1S\_1032 (10-fold) and A1S\_1033 (8-fold), respectively. Major transcriptional differences were also observed in the ‘posttranslational modification, protein turnover and chaperone’ COG. Approximately 7% of the 117 genes within this group were down-regulated more than 4-fold. A gene within this class encoding Lon protease (A1S\_1030) was approximately 10-fold down-regulated. Lon proteases have shown to be involved in regulation of QS-signals (Bertani *et al.* 2007). Interestingly, the homoserine lactone synthase (A1S\_0109) and the homoserine lactone responsive regulator (A1S\_0111), were heavily up-regulated (Figure 5.7). The *A. baumannii* signal transduction system will be further discussed in Section 5.2.6.

## 5.2.5 Examination of metabolic differences

### 5.2.5.1 Expression levels of *paaA*

A number genes functioning in metabolism were significantly down-regulated in strain 17978hm as compared to WT cells. Motile cells may have the ability to migrate to more nutrient rich areas of the agar plate, whereas non-motile cells would grow on the inoculated sites only. Therefore, in this study, non-motile cells may have been investigated under partially nutrient-limiting conditions compared to motile cells. This could have resulted in up-regulation of various metabolic pathways in strain ATCC 17978 in an attempt to utilise alternative carbon sources (Appendix E). Major transcriptional differences were observed in the *paa* cluster (A1S\_1335-1349; Figure 5.8), which is involved in phenylacetic acid degradation. Furthermore, a benzoate transportation system (A1S\_1867-1869) and a Glu-tRNA amidotransferase (A1S\_1865) were also heavily down-regulated. Glu-tRNA amidotransferase plays a putative role in styrene degradation, aminobenzoate degradation and phenylalanine metabolism.

The possibility that nutrient deficiency resulted in the transcriptome differences observed in genes with a putative function in metabolism was further investigated. Transcription levels of *paaA* (A1S\_1336) were examined in broth cultures and in

cells grown on semi-solid LB media by qRT-PCR analysis (Section 2.4.15) using the A1S\_1336 specific oligonucleotides listed in Table 2.4. Interestingly, transcription levels of cells isolated from semi-solid LB media were similar to that observed for cells isolated from semi-solid MH media, *viz.* more than 100-fold higher in WT cells compared to 17978hm cells (data not shown). Both WT and 17978hm cells are motile on semi-solid LB media, therefore, up-regulation of *paaA* in WT cells appears to not be directly related to nutrient deficiency. Expression levels of *paaA* were low in both strains when cultured in liquid media, indicating that strain 17978hm may have an impaired ability to overexpress the *paa* gene cluster (data not shown).

#### 5.2.5.2 Carbon source utilisation

The growth rate in nutrient rich media, such as MH, was shown to be similar between the two strains (Figure 5.2), however, minor differences were observed using minimal medium (M9) supplemented with either glucose or phenanthrene (data not shown). Therefore, a Phenotype MicroArray™ (BIOLOG, Inc.) analysis was performed to obtain a comprehensive depiction of carbon source utilisation by strains 17978hm and WT (Section 2.3.8). The Phenotype MicroArray™ allows investigation of metabolic activity under different environmental conditions by measuring the respiration using redox chemistry ([www.biolog.com](http://www.biolog.com)). MicroPlate™ PM1 and PM2A together contain 190 different carbon sources (Figure 5.9). WT cells showed slightly higher respiratory levels in the presence of multiple different carbon sources. However, the most pronounced dissimilarities were observed in the presence of L-threonine or D-malic acid, in which WT cells showed more active respiration than 17978hm cells (Figure 5.9). Interestingly, the transcriptomic analysis revealed up-regulation of a gene encoding a putative amino acid efflux protein (RhtB/LysE; A1S\_3397) (Figure 5.12; Appendix D), which may have resulted in reduced levels of intracellular L-threonine.

Utilisation of D-malic acid as a carbon source requires tartrate/D-malate dehydrogenase (A1S\_0849) which converts D-malic acid into pyruvate (Reed *et al.* 2006). Transcriptomic analysis revealed that A1S\_0849 was transcribed at slightly lower levels in strain 17978hm compared to WT cells (~1.4-fold). However, this reduction may be compensated for by the high levels of overexpression observed in genes encoding enzymes involved in conversion of pyruvate to acetyl-CoA (A1S\_1698-1704) in strain 17978hm (Appendix D). Pyruvate was utilised at similarly high levels in both strains. Various genes encoding proteins functioning in

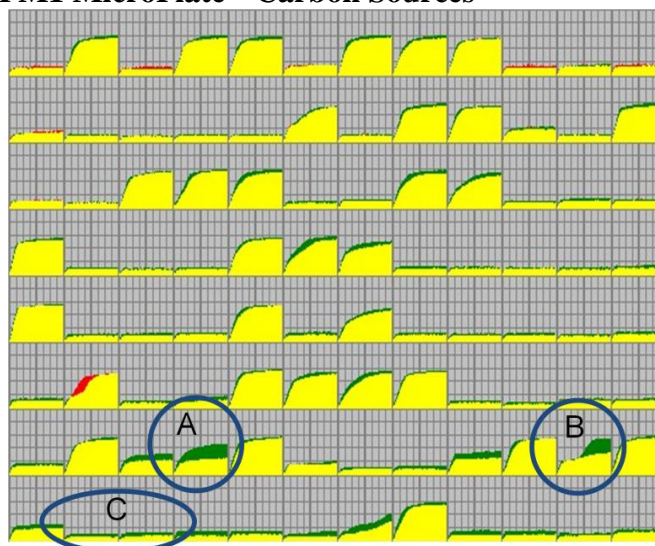
**PM1 MicroPlate™ Carbon Sources**

A1 Negative Control	A2 L-Arabinose	A3 N-Acetyl-D-Glucosamine	A4 D-Saccharic Acid	A5 Succinic Acid	A6 D-Galactose	A7 L-Aspartic Acid	A8 L-Proline	A9 D-Alanine	A10 D-Trehalose	A11 D-Mannose	A12 Dulcitol
B1 D-Serine	B2 D-Sorbitol	B3 Glycerol	B4 L-Fucose	B5 D-Gluconic Acid	B6 D-Gluconic Acid	B7 D,L- $\alpha$ -Glycerol-Phosphate	B8 D-Xylose	B9 L-Lactic Acid	B10 Formic Acid	B11 D-Mannitol	B12 L-Glutamic Acid
C1 D-Glucose-6-Phosphate	C2 D-Galactonic Acid- $\gamma$ -Lactone	C3 D,L-Malic Acid	C4 D-Ribose	C5 Tween 20	C6 L-Rhamnose	C7 D-Fructose	C8 Acetic Acid	C9 $\alpha$ -D-Glucose	C10 Maltose	C11 D-Melibiose	C12 Thymidine
D-1 L-Asparagine	D2 D-Aspartic Acid	D3 D-Glucoaminic Acid	D4 1,2-Propanediol	D5 Tween 40	D6 $\alpha$ -Keto-Glutaric Acid	D7 $\alpha$ -Keto-Butyric Acid	D8 $\alpha$ -Methyl-D-Galactoside	D9 $\alpha$ -D-Lactose	D10 Lactulose	D11 Sucrose	D12 Uridine
E1 L-Glutamine	E2 M-Tartaric Acid	E3 D-Glucose-1-Phosphate	E4 D-Fructose-6-Phosphate	E5 Tween 80	E6 $\alpha$ -Hydroxy Glutaric Acid- $\gamma$ -Lactone	E7 $\alpha$ -Hydroxy Butyric Acid	E8 $\beta$ -Methyl-D-Glucoside	E9 Adonitol	E10 Maltotriose	E11 2-Deoxy Adenosine	E12 Adenosine
F1 Glycyl-L-Aspartic Acid	F2 Citric Acid	F3 M-Inositol	F4 D-Threonine	F5 Fumaric Acid	F6 Bromo Succinic Acid	F7 Propionic Acid	F8 Mucic Acid	F9 Glycolic Acid	F10 Glyoxylic Acid	F11 D-Cellobiose	F12 Inosine
G1 Glycyl-L-Glutamic Acid	G2 Tricarballic Acid	G3 L-Serine	G4 L-Threonine	G5 L-Alanine	G6 L-Alanyl-Glycine	G7 Acetoacetic Acid	G8 N-Acetyl- $\beta$ -D-Mannosamine	G9 Mono Methyl Succinate	G10 Methyl Pyruvate	G11 D-Malic Acid	G12 L-Malic Acid
H1 Glycyl-L-Proline	H2 $\alpha$ -Hydroxy Phenyl Acetic Acid	H3 $\alpha$ -Hydroxy Phenyl Acetic Acid	H4 Tyramine	H5 D-Palcoee	H6 L-Xylose	H7 Glucuronamide	H8 Pyruvic Acid	H9 L-Galactonic Acid- $\gamma$ -Lactone	H10 D-Galacturonic Acid	H11 Phenylethyl-amine	H12 2-Aminoethanol

**PM2A MicroPlate™ Carbon Sources**

A1 Negative Control	A2 Chondroitin Sulfate C	A3 $\alpha$ -Cyclodextrin	A4 $\beta$ -Cyclodextrin	A5 $\gamma$ -Cyclodextrin	A6 Dextrin	A7 Gelatin	A8 Glycogen	A9 Inulin	A10 Laminarin	A11 Mannan	A12 Pectin
B1 N-Acetyl-D-Galactosamine	B2 N-Acetyl-Neuraminic Acid	B3 $\beta$ -D-Aliose	B4 Amygdalin	B5 D-Arabinose	B6 D-Arabitol	B7 L-Arabitol	B8 Arbutin	B9 2-Deoxy-D-Ribose	B10 I-Erythritol	B11 D-Fucose	B12 3-O- $\beta$ -D-Galactopyranosyl-D-Arabinose
C1 Gentibiose	C2 L-Glucose	C3 Lactitol	C4 D-Melezitose	C5 Maltitol	C6 $\beta$ -Methyl-D-Glucoside	C7 $\beta$ -Methyl-D-Galactoside	C8 $\beta$ -Methyl Glucose	C9 $\beta$ -Methyl-D-Gluconic Acid	C10 $\alpha$ -Methyl-D-Mannoside	C11 $\beta$ -Methyl-D-Xyloside	C12 Palatinose
D1 D-Raffinose	D2 Salicin	D3 Sedoheptulosan	D4 L-Sorbose	D5 Stachyose	D6 D-Tagatose	D7 Turanose	D8 Xylitol	D9 N-Acetyl-D-Glucosaminitol	D10 $\gamma$ -Amino Butyric Acid	D11 $\delta$ -Amino Valeric Acid	D12 Butyric Acid
E1 Capric Acid	E2 Caproic Acid	E3 Citraconic Acid	E4 Citramalic Acid	E5 D-Glucosamine	E6 2-Hydroxy Benzolic Acid	E7 4-Hydroxy Benzolic Acid	E8 $\beta$ -Hydroxy Butyric Acid	E9 $\gamma$ -Hydroxy Butyric Acid	E10 $\alpha$ -Keto-Valeric Acid	E11 Itaconic Acid	E12 5-Keto-D-Gluconic Acid
F1 D-Lactic Acid Methyl Ester	F2 Malonic Acid	F3 Melibionic Acid	F4 Oxalic Acid	F5 Oxalomalic Acid	F6 Quinic Acid	F7 D-Ribono-1,4-Lactone	F8 Sebaic Acid	F9 Sorbic Acid	F10 Succinamic Acid	F11 D-Tartaric Acid	F12 L-Tartaric Acid
G1 Acetamide	G2 L-Alaninamide	G3 N-Acetyl-L-Glutamic Acid	G4 L-Arginine	G5 Glycine	G6 L-Histidine	G7 L-Homoserine	G8 Hydroxy-L-Proline	G9 L-Isoleucine	G10 L-Leucine	G11 L-Lysine	G12 L-Methionine
H1 L-Omitiline	H2 L-Phenylalanine	H3 L-Pyrogultamic Acid	H4 L-Valine	H5 D,L-Carnitine	H6 Sec-Butylamine	H7 D,L-Octopamine	H8 Putrescine	H9 Dihydroxy Acetone	H10 2,3-Butanediol	H11 2,3-Butanone	H12 3-Hydroxy 2-Butanone

### PM1 MicroPlate™ Carbon Sources



### PM2A MicroPlate™ Carbon Sources

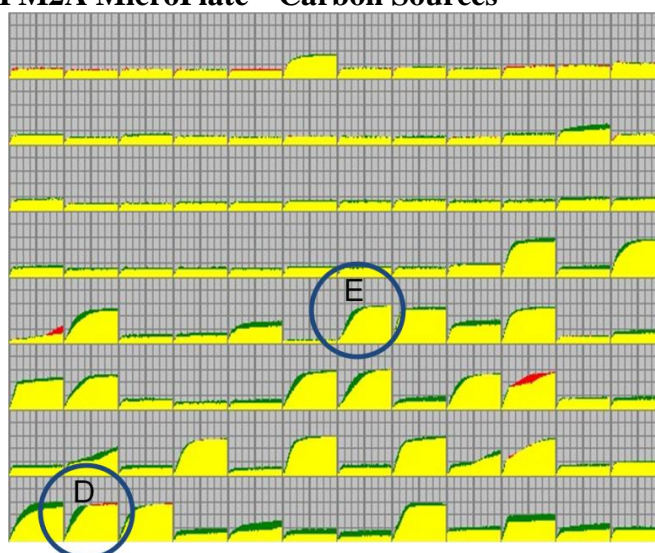


**Figure 5.9: Comparative analysis of carbon source utilisation**

The respiratory activity in the presence of 190 different carbon sources was investigated for 72 hours using Phenotype MicroArray™ (BIOLOG, Inc.) analysis of two MicroPlates™, PM1 (top) and PM2A (bottom) (Section 2.3.8). The name of the carbon source analysed per well has been provided in the tables (on the left-hand side page) in the respective positions. Activity of ATCC 17978 cells is depicted in green and that of 17978hm cells in red, the overlay of the two strains has been shown in yellow. Activity was similar under most conditions, however, activity of ATCC 17978 cells was considerably higher than that of 17978hm cells when incubated in the presence of L-threonine (A) or D-malic acid (B). Phenylalanine (D), benzoic acid (E) and m- and p-hydroxy phenylacetic acid (C) have been indicated, as major transcriptional differences were observed for genes involved in metabolism of these compounds (Appendices D and E).

L-malic acid metabolism were significantly underexpressed in 17978hm cells, such as malate synthase G (A1S\_1601) and malate dehydrogenase (A1S\_3025). Nevertheless, L-malic acid and a combination of D- and L-malic acid was efficiently utilised as a carbon source by both strains (Figure 5.9).

Various genes of the butanoate metabolism pathway were up-regulated in the 17978hm strain. This includes A1S\_1704 which encodes an acetoin dehydrogenase responsible for conversion of acetoin to 2,3-butanediol. Whereas A1S\_1704 showed 4-fold up-regulation in strain 17978hm (Appendix D), the gene encoding butanediol dehydrogenase (A1S\_1705) is similarly expressed in both cultures. This may result in accumulation of 2,3-butanediol. WT cells showed slightly more activity when grown with 2,3-butanediol as the sole carbon source compared to 17978hm (Figure 5.9). However, a link between impaired 2,3-butanediol utilisation and the phenotypic alterations of strain 17978hm could not be established.

The Phenotype MicroArray™ results showed that phenylalanine was used as a carbon source by both strains (Figure 5.9). Interestingly, in the same analysis it was shown that neither WT nor 17978hm cells showed active respiration in the presence of phenylacetic acid, which is one of the catabolic products of phenylalanine. The genes encoding proteins required for catabolism of phenylalanine to phenylacetic acid were all down-regulated in strain 17978hm (Appendix E). Regardless, the use of phenylalanine as a carbon source appears to be independent of the catabolic pathway utilising the *paa* cluster. Instead, phenylalanine is potentially converted to benzoic acid, which can be used as a carbon source by both strains (Figure 5.9). The analysis of the carbon source utilisation profiles of strains ATCC 17978 and 17978hm did not reveal a putative function of the *paa* cluster. Noteworthy, the *paa* cluster in the WT strain was only up-regulated under motile conditions and not when cultured in broth (Section 5.2.5.1). It can not be ruled out that different pathways are being utilised in nutrient-rich media instead of the minimal media used for Phenotype MicroArray™ analysis.

## 5.2.6 Signal transduction in *A. baumannii*

Many different multicellular bacterial modes of living require QS-signals, such as life in a biofilm or communal migration (Daniels *et al.* 2004; de Kievit 2009). In *A. baumannii* a role for QS in biofilm formation and pellicle formation has been shown (Niu *et al.* 2008). This signal transduction system is mediated by acyl

homoserine lactones (AHLs) (Bhargava *et al.* 2010; Gonzalez *et al.* 2009; Gonzalez *et al.* 2001; Niu *et al.* 2008). AHLs of varying lengths have been identified and 74% of clinical *A. baumannii* strains were found to produce one or more different QS-signals (Gonzalez *et al.* 2009; Gonzalez *et al.* 2001). In the transcriptomic analysis conducted here, the gene cluster responsible for QS-signal biosynthesis was found to be heavily up-regulated in the motile population. Expression levels of one of the genes within this cluster, *abaI*, were investigated in *A. baumannii* ATCC 17978 and 17978hm grown on semi-solid LB media by qRT-PCR (Section 2.4.15) using the *abaI* (A1S\_0109) specific oligonucleotides (Table 2.4). Both strains displayed a motile zone after incubation for 8 hours and qRT-PCR analysis of these cells harvested using the same method as described for transcriptome analysis (Section 5.2.4.1) showed that *abaI* expression was at levels similar to that found in motile 17978hm cells grown on semi-solid MH media (data not shown). Therefore, up-regulation of QS-signal biosynthesis genes under motile conditions on semi-solid LB agar is not a feature restricted to the hyper-motile variant strain.

#### **5.2.6.1 The genomic organisation of the region harbouring the quorum-sensing signal biosynthesis cluster**

The *A. baumannii* ATCC 17978 AHL biosynthesis gene cluster contains *abaI* (A1S\_0109), which encodes the homoserine lactone synthase, an ORF encoding a protein of unknown function (A1S\_0110) and *abaR* (A1S\_0111), which encodes a regulatory protein (Figure 5.10). The genomic organisation and amino acid sequences share high homology with the QS-signal biosynthesis clusters of many other bacteria, such as *Burkholderia pseudomallei* (Niu *et al.* 2008).

A locus containing eight ORFs (A1S\_0112-0119) is located adjacent to *abaR* (Figure 5.10). The genes within this cluster were up-regulated more than 100-fold in strain 17978hm, levels higher than observed for *abaI* and *abaR*. This cluster has been predicted to function in biosynthesis of secondary metabolites, such as lipopeptides and/or polyketides (Clemmer *et al.* 2011). Two genes within this cluster encode proteins with a predicted function in transport of the synthesised molecules to the extracellular space (A1S\_0116-0117). A1S\_0116 encodes a predicted member of the RND superfamily (Table 6.1). RND proteins form trimers in the inner-membrane and function as translocators of compounds from the cytoplasm or periplasm (Section 1.3.4.5). A1S\_0117 encodes a putative outer membrane porin protein,

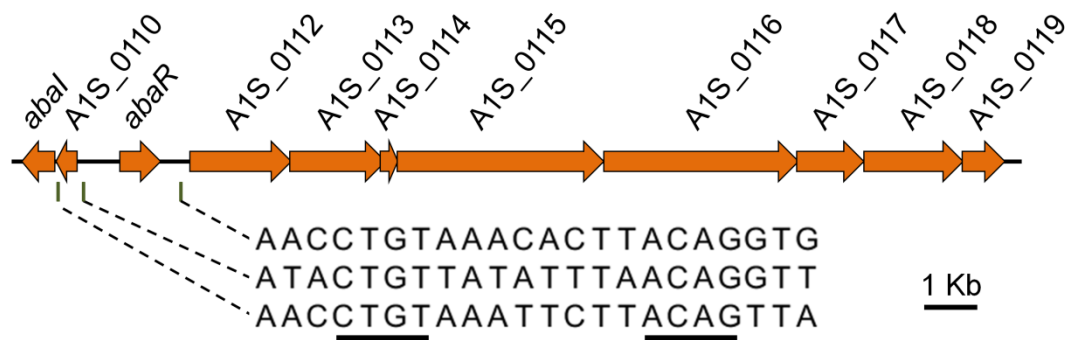


**Figure 5.10: Genetic organisation of *A. baumannii* QS-regulated genes**

The genes depicted in this figure were all highly up-regulated in the motile population. Putative AbaR binding sites were identified using a bioinformatics approach (Section 2.7.3). The first binding site was located upstream from the gene encoding homoserine lactone synthase, *abaI* (A1S\_0109). The second putative AbaR binding site was identified upstream from A1S\_0110, a gene encoding a protein of unknown function. The third site was found upstream from A1S\_0112, the start of a large operon involved in biosynthesis of lipopeptides and/or polyketides. The fully conserved nucleotide sequences of the inverted repeats have been underlined.

which was identified using a Blastp search, and may function as the facilitator of secretion of the synthesised secondary metabolites to the extracellular space.

In this study, comparative genomic analyses were conducted using Mauve (Section 2.7.2). This showed that the QS-signal biosynthesis cluster and the large adjacent operon, were well conserved between most fully sequenced *A. baumannii* isolates (data not shown). However, both *abaI* and *abaR*, and the majority of the adjacent operon had been removed by an insertion element in the non-pathogenic *A. baumannii* strain SDF and *abaR* had been disrupted by an insertion element in *A. baumannii* strain 1656-2 (data not shown). Interestingly, strain 1656-2 has previously been described as having a particularly high level of biofilm production (Shin *et al.* 2009). The role of AbaR requires further investigation, as AbaR homologues, such as LuxR, have been found to transcriptionally activate genes encoding homoserine lactone synthase (Waters and Bassler 2005), *abaI* in the case of *A. baumannii*. Therefore, inactivation of *abaR* is expected to result in the reduction of QS-signal production and consequently reduced levels of biofilm formation.

The 54 clinical *A. baumannii* isolates in our collection (Table 2.2) were examined for the presence of A1S\_0116 by PCR (Section 2.4.14) using oligonucleotides specific to A1S\_0116 (Table 2.4). Whereas all international clone I isolates were positive, less than 25% of international clone II isolates harboured A1S\_0116 (Section 6.2.1; Table 6.1). No direct correlation could be established between presence or absence of A1S\_0116 and the level of biofilm formation or motility characteristics as determined in Sections 4.2.3 and 4.2.2, respectively.

### 5.2.6.2 Investigation of AbaR binding sites

AbaR is activated upon exposure to AHLs and subsequently induces expression of *abaI* (Bhargava *et al.* 2010; Waters and Bassler 2005). In many other bacteria, AbaR homologues, such as LuxR, are known to regulate other genes functioning in processes such as iron acquisition or virulence (Cornelis *et al.* 2009; Daniels *et al.* 2004; de Kievit 2009; Shao *et al.* 2011). In *Acinetobacter*, AbaR has been shown to regulate *abaI*, and A1S\_0113 and A1S\_0115 from the adjacent operon (Clemmer *et al.* 2011; Niu *et al.* 2008). To investigate other potential regulatory targets of AbaR, the AbaR binding sites in the ATCC 17978 genome were investigated using a bioinformatics approach, which included the MEME suite (Section 2.7.3). The AbaR binding site identified upstream of *abaI* (CTGTAAATTCTTACAG) showed high

levels of homology with the well-characterised *Vibrio fischeri* lux box (Antunes *et al.* 2008; Niu *et al.* 2008). Therefore, all 11 positively identified *V. fischeri* LuxR binding sites were included to create a comprehensive scoring matrix using the MEME suite (Bailey and Elkan 1994; Bailey and Gribskov 1998). The scoring matrix was subsequently aligned to the *A. baumannii* ATCC 17978 genome using MAST. The transcriptional up-regulation of all genes with a putative AbaR binding site was examined using the transcriptomic data obtained in this study (Appendix D and E). Three sites showed both a high level of homology to the scoring matrix and major differential expression levels (Figure 5.10). This included the previously identified sequence in the upstream region of *abaI*, but also a site located in the intergenic region between A1S\_0110 and *abaR* (A1S\_0111), and a site upstream of A1S\_0112, the first ORF of the operon which includes A1S\_0113 and A1S\_0115 (Clemmer *et al.* 2011). Although AbaR auto-regulation has been described in other bacteria such as *V. fischeri*, the putative AbaR binding site in *A. baumannii* ATCC 17978 is located 680 bp upstream of *abaR*, creating uncertainties about its regulatory influence. Nevertheless, transcriptional activation of A1S\_0110 and *abaR* was at similar levels in the motile population. All three putative binding sites are entirely conserved between the fully sequenced *A. baumannii* isolates that contain the AHL biosynthesis gene cluster (data not shown). Sequence homology of the scoring matrix to other putative AbaR binding site sequences was significantly lower than that observed in the three sites described above (data not shown). Alternatively, putative AbaR binding sites were found to be located within an ORF instead of in the regulatory region of a gene. An optimised *A. baumannii* AbaR binding site scoring matrix was generated using the three binding sites sequences. However, feasible AbaR binding sites outside the QS-signal biosynthesis cluster were not identified in the ATCC 17978 genome when taking the same bioinformatic approach as described above (data not shown).

### 5.2.6.3 *Lon* protease

A gene encoding a putative Lon protease (A1S\_1030) was found to be down-regulated in strain 17978hm by more than 10-fold (Section 5.2.4.2; Appendix E). Although *lon* was found to be overexpressed in *A. baumannii* upon induction with ethanol (Camarena *et al.* 2010), the function of Lon proteases in *A. baumannii* has not been reported. In other bacteria, Lon has been described as an ATP-dependent protease that plays a major role in degradation of endogenous proteins (Laskowska *et*

*al.* 1996). The *P. aeruginosa* and *E. coli* Lon proteases appear to have a broad substrate range and are therefore involved in regulatory control of many different processes in the cell (Van Melderen and Aertsen 2009). In *P. aeruginosa*, Lon protease has also been shown to reduce QS-signal production by proteolysis of LasI, an AHL synthase (Takaya *et al.* 2008). Interestingly, the *Pseudomonas putida* Lon protease was shown to degrade RsaR, a regulator of the AHL biosynthesis genes (Bertani *et al.* 2007). Disruption of *lon* in *P. aeruginosa* was shown to negatively affect biofilm formation, swimming, swarming and twitching (Marr *et al.* 2007). Expression of *lon* was induced in *P. aeruginosa* upon exposure to aminoglycosides, potentially affecting the expression of virulence determinants (Marr *et al.* 2007). *E. coli lon* negative mutants over-produced exopolysaccharides, which subsequently played a crucial role in protection from desiccation (Brill *et al.* 1988; Gottesman and Stout 1991; Ophir and Gutnick 1994; Trisler and Gottesman 1984). Overall, the down-regulation of *lon* observed in *A. baumannii* strain 17978hm (Appendix E) indicates that QS-signal production and consequently various persistence and virulence mechanisms may be expressed at even higher levels in strain 17978hm.

### **5.2.7 Genome sequence analysis of *A. baumannii* strains ATCC 17978 and 17978hm**

The genome of both strain 17978hm and ATCC 17978 were sequenced to assess their genetic differences. Cells of both strains were grown ON on semi-solid MH media and the DNA was isolated (Section 2.4.2). The genomes of the WT and 17978hm strains were sequenced using Illumina BeadArray technology (Section 2.4.7). The sequence reads were assembled using Velvet 1.1 (Zerbino and Birney 2008), generating 245 contigs for strain 17978hm and 292 contigs for strain ATCC 17978. The total length was 4,084,591 bp (65-fold coverage) and 4,067,428 bp (94-fold coverage) for strain 17978hm and ATCC 17978, respectively. Whole genome alignments were generated using Mauve (Section 2.7.2), the ‘original’ ATCC 17978 genome sequence (CP000521) was included for comparative purposes.

#### **5.2.7.1 Single nucleotide polymorphisms**

After removal of poor sequence reads, represented by ‘N’, more than 400 SNPs were identified by Mauve (Section 2.7.2) when comparing the 17978hm genome to either the WT genome or CP000521 (data not shown). Approximately the same number of SNPs were identified when comparing the ATCC 17978 genome to CP000521 (data not shown). Therefore, only the SNPs identified in the 17978hm

sequence when compared to both the WT and CP000521 genome sequences were further analysed (Table 5.1). The 44 SNPs identified were divided over only 12 ORFs, 17 of these, located in A1S\_1201, A1S\_1893 and A1S\_1849, were found to be errors in the genome sequence by Sanger sequencing using the oligonucleotides specific to these ORFs (Section 2.4.7; Table 5.1). Noteworthy, many SNPs identified here were located in regions that were originally incorrectly sequenced in CP000521, leading to incorrect annotation of the ORFs (data not shown). Poor sequencing and consequently incorrect ORF annotation has also been observed for a gene encoding a RND drug transporter *adeM* (A1S\_3445/6) (Section 6.2.1). This indicated that certain regions of the *A. baumannii* ATCC 17978 genome may be difficult to sequence using either Illumina BeadArray technology (Section 2.4.7) or pyrosequencing (Smith *et al.* 2007). A SNP identified in A1S\_3222 was confirmed in this study (Table 5.1); A1S\_3222 encodes a putative O-acetyl-L-homoserine acetate-lyase, which functions in biosynthesis of methionine and cysteine. The SNP results in replacement of a leucine to an arginine in position 360 (based on AB013613), which is not located within any known conserved domains (Section 2.7.2) (data not shown). Significantly, a second hyper-motile clone was identified in a mutant library (as part of another study) of *A. baumannii* strain ATCC 17978 generated by using a mini-Tn10 transposon. To date, the location of the mini-Tn10 transposon insertion in this strain, named *A. baumannii* B23 (Table 2.2), has not been defined. However, the SNP in A1S\_3222 was not present in *A. baumannii* strain B23. Therefore, the mutation in A1S\_3222 in strain 17978hm is unlikely to play a role in the hyper-motile phenotype of strains 17978hm and B23.

#### **5.2.7.2 Insertional inactivation of a gene encoding a putative histone-like protein**

The whole genome alignment of strain 17978hm, ATCC 17978 and CP000521 was also used to identify genetic material unique to strain 17978hm. Of major significance was an insertion element found only in A1S\_0268 of strain 17978hm. Eight nucleotides of the A1S\_0268 target sequence were duplicated and flanked the termini of the insertion element (Figure 5.11). The insertion sequence appeared to have been generated by a duplication event of A1S\_0628, as a Blastn search showed 100% identity between the insertion sequence found in A1S\_0268 in strain 17978hm and the insertion sequence containing A1S\_0628. Two other sequences found in strain 17978hm and ATCC 17978, A1S\_2554 and A1S\_1172 showed 97% and 84% sequence homology to A1S\_0628, respectively. Interestingly, *A. baumannii* strain

**Table 5.1: Single nucleotide polymorphisms identified in the *A. baumannii* 17978hm genome**

<b>SNP pattern <sup>a</sup></b>	<b>Position of SNP <sup>b</sup></b>	<b>Locus-tag</b>	<b>Gene function</b>	<b>Sanger sequencing results <sup>c</sup></b>
AGG	1406236	A1S_1201	Alkyl hydroperoxide reductase	Rebutted
TCC	1406311	A1S_1201	Alkyl hydroperoxide reductase	Rebutted
AGG	1406317	A1S_1201	Alkyl hydroperoxide reductase	Rebutted
TCC	1406399	A1S_1201	Alkyl hydroperoxide reductase	Rebutted
AGG	1406411	A1S_1201	Alkyl hydroperoxide reductase	Rebutted
AGG	1406420	A1S_1201	Alkyl hydroperoxide reductase	Rebutted
AGG	1406477	A1S_1201	Alkyl hydroperoxide reductase	Rebutted
AGG	1406615	A1S_1201	Alkyl hydroperoxide reductase	Rebutted
TCC	1406630	A1S_1201	Alkyl hydroperoxide reductase	Rebutted
CTT	2148400	A1S_1893	Benzoate degradation	Rebutted
TCC	2148403	A1S_1893	Benzoate degradation	Rebutted
CTT	2148421	A1S_1893	Benzoate degradation	Rebutted
GCC	2194864	A1S_1894	Benzoate degradation	Rebutted
GTT	3108494	A1S_2682	Cell division	nd
GTA	2149473	A1S_1849	EC:2.3.1.9	Rebutted
ATT	2149474	A1S_1849	EC:2.3.1.9	Rebutted
AGG	2149865	A1S_1849	EC:2.3.1.9	Rebutted
GAA	2149926	A1S_1849	EC:2.3.1.9	Rebutted
GAA	2193445	A1S_1891	EC:2.3.1.9	nd
TAA	2193461	A1S_1891	EC:2.3.1.9	nd
ATT	1334207	A1S_3604	Hypothetical	nd
ATT	1334365	A1S_3604	Hypothetical	nd

<b>SNP pattern</b> <sup>a</sup>	<b>Position of SNP</b> <sup>b</sup>	<b>Locus-tag</b>	<b>Gene function</b>	<b>Sanger sequencing results</b> <sup>c</sup>
GAA	1336571	A1S_1143	Hypothetical	nd
CTT	1336572	A1S_1143	Hypothetical	nd
AGG	1336577	A1S_1143	Hypothetical	nd
GAA	1336580	A1S_1143	Hypothetical	nd
GTT	3713698	A1S_3222	O-acetyl-L-homoserine acetate-lyase	Confirmed (L360R) <sup>d</sup>
AGG	2368690	A1S_3771	Phage-like protein	nd
AGG	3582922	A1S_3104	RNA helicase	nd
TCC	300986	A1S_0279	Translation elongation factor	nd
AGG	2950133	A1S_2554	Transposase-like	nd
TCC	2950192	A1S_2554	Transposase-like	nd
AGG	2950436	A1S_2554	Transposase-like	nd
GTT	2950454	A1S_2554	Transposase-like	nd
GAA	2950516	A1S_2554	Transposase-like	nd
GAA	2950655	A1S_2554	Transposase-like	nd
ACC	2950676	A1S_2554	Transposase-like	nd
GAA	2950677	A1S_2554	Transposase-like	nd
GAA	2950682	A1S_2554	Transposase-like	nd
ACC	2950912	A1S_2554	Transposase-like	nd
CTT	2950914	A1S_2554	Transposase-like	nd
TCC	2950920	A1S_2554	Transposase-like	nd
GAA	2950932	A1S_2554	Transposase-like	nd
ACC	2951022	A1S_2554	Transposase-like	nd

<sup>a</sup> The nucleotides represent, from left to right; 17978hm, ATCC 17978 and CP000521.

<sup>b</sup> Based on the CP000521 sequence.

<sup>c</sup> nd = not determined.

<sup>d</sup> Leucine to arginine in amino acid position 360, based on AB013613.

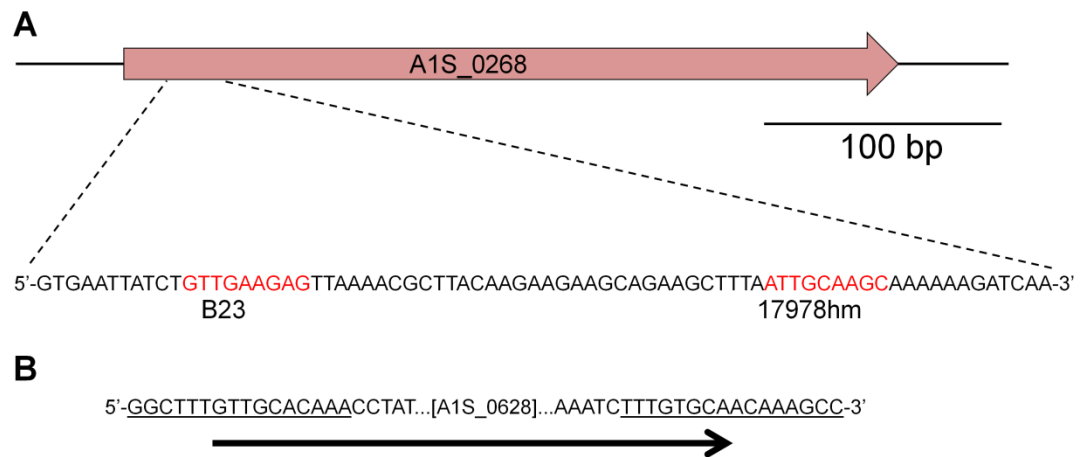


**Figure 5.11: Positioning of the insertion elements identified in A1S\_0268 of *A. baumannii* strains 17978hm and B23**

Using whole genome sequencing of the WT and 17978hm strains, an insertion element (B) was identified in a position unique to *A. baumannii* strain 17978hm as compared to the WT genome (A). The same insertion sequence, most likely originating from a duplication event of a mobile genetic element containing A1S\_0628, was also identified in strain B23 using Sanger sequencing (A). The sequence of the WT ORF has been provided (A), the target sites of the insertion sequence are shown in red and the inverted repeats part of the insertion element have been underlined (B). The orientation of the insertion sequence was the same in both mutants, indicated by the black arrow.

B23, the hyper-motile clone identified in a mutant library of strain ATCC 17978 (Section 5.2.7.1), was found to contain the same insertion element, originated from A1S\_0628, in A1S\_0268. However, the position and target site of the insertion sequence in A1S\_0268 in strain B23 is different to that of strain 17978hm (Figure 5.11). As mentioned previously, the location of the mini-Tn10 transposon in strain B23 introduced by generating the mutant library is currently unknown. Overall, these results indicated that the insertion element identified in strain 17978hm may duplicate and disrupt other regions within the *A. baumannii* ATCC 17978 genome at a relatively high rate. There is no evidence that A1S\_0268 is a preferred target site for the insertion element, this insertion may occur randomly, and was picked-up as identification of hyper-motile variants is relatively straightforward (Figure 5.1).

The transcriptomic data of *A. baumannii* strain ATCC 17978 and 17978hm grown on semi-solid MH media (Section 5.2.4) correlated with the findings of a duplication event of the mobile genetic element containing an ORF encoding a transposase (A1S\_0628). The transposase gene A1S\_0628, which was identified as inactivating A1S\_0268, was highly up-regulated in strain 17978hm (>40-fold; Appendix D). This could not be explained simply by the duplication of the mobile genetic element containing A1S\_0628. However, the site of integration was within a gene (A1S\_0268) that was highly transcriptionally active in both strains ATCC 17978 and 17978hm, as determined by microarray (Table 5.2). Therefore, the transcriptionally active target site may have contributed to the more than 40-fold increase in mRNA transcripts of A1S\_0628. The transcriptomic data also revealed up-regulation of A1S\_2554 and A1S\_1172 (Appendix D). This is likely to be a result of unspecific binding of the A1S\_0628 transcripts to the probes of these highly similar ORFs.

The WT A1S\_0268 gene encodes a putative H-NS protein of the histone-like protein family. The H-NS proteins are global repressor proteins and preferentially bind AT-rich DNA sequences (Lang *et al.* 2007; Rimsky 2004). Spontaneous insertional inactivation of H-NS has also been observed in other bacteria, such as *Mycobacterium smegmatis* (Arora *et al.* 2008). Some of the phenotypic alterations reported for the *M. smegmatis* H-NS mutant strain were similar to that of strain *A. baumannii* 17978hm, e.g. displaying hyper-motility. As mentioned above, H-NS preferentially binds AT-rich DNA and horizontally-acquired genetic material is often AT-rich and is therefore a likely target for H-NS proteins. A common example of a

**Table 5.2: Signal strengths of A1S\_0268 and A1S\_0628 in *A. baumannii* strains ATCC 17978 and 17978hm determined by microarray**

	A1S_0268		A1S_0628	
	ATCC 17978	17978hm	ATCC 17978	17978hm
<b>RFU</b> <sup>a</sup>	21219	39427	3092	121698

<sup>a</sup> Average fluorescent signal strength in relative fluorescent units (RFU), determined by microarray (Section 2.5).

horizontally-acquired genomic region targeted by H-NS encodes the type VI secretion system (Bernard *et al.* 2010). Indeed, this cluster was found to be heavily up-regulated in strain 17978hm (Appendix D; Figure 5.7). Other potential regulatory targets of the *A. baumannii* H-NS protein were identified using the CGView server (Grant and Stothard 2008). The *A. baumannii* ATCC 17978 genome was used as a template and the transcriptomic data obtained in this study were processed to allow incorporation into the circular representation of the genome (Figure 5.12). Furthermore, to identify horizontally-acquired genetic material, Blastn analysis of three additional *A. baumannii* genomes was included; AYE, ACICU and WM99c. A correlation between non-conserved regions and transcriptional up-regulation was observed, e.g. various regions not identified in all four genomes were more than 2-fold up-regulated in strain 17978hm (Figure 5.12). Of predominant interest were a surface protein (A1S\_0745), an autotransporter adhesin (A1S\_1032) and a putative antigen (A1S\_1033). These surface presented proteins may play a role in the phenotypic alterations observed for strain 17978hm. Transcription of a gene encoding the *E. coli* autotransporter protein UpaC was recently found to be transcriptionally repressed by H-NS (Allsopp *et al.* 2011), this corroborates the data obtained in this study using a bioinformatics approach. The S-adenosyl-L-methionine (SAM)-dependent methyltransferase (A1S\_2744), also potentially regulated by H-NS (Figure 5.12), is involved in methylation of proteins, lipids, DNA and RNA, therefore, controlling a wide range of cellular processes (Sun *et al.* 2005). As mentioned in Section 5.2.5.2, a putative homoserine/threonine (RhtB) or lysine (LysE) resistance mechanism was up-regulated (A1S\_3397; Appendix D). A1S\_3379 was not found in strain AYE, ACICU or WM99c and is therefore also a potential target for transcriptional repression by H-NS. A strong correlation between the GC-percentage and the transcriptome results was not observed. This may be due to the in general low GC-percentage of the *A. baumannii* ATCC 17978 genome (~39%).

### 5.2.7.3 *Complementation assays*

To confirm that the altered phenotypes observed in *A. baumannii* 17978hm and B23 were a result of inactivation of A1S\_0268, WT A1S\_0268 was introduced in these H-NS null mutants. The A1S\_0268 ORF and 200 bp of the upstream region was isolated from strain ATCC 17978 by PCR using the A1S\_0268 oligonucleotides (Table 2.4). The amplified product was subsequently cloned into the

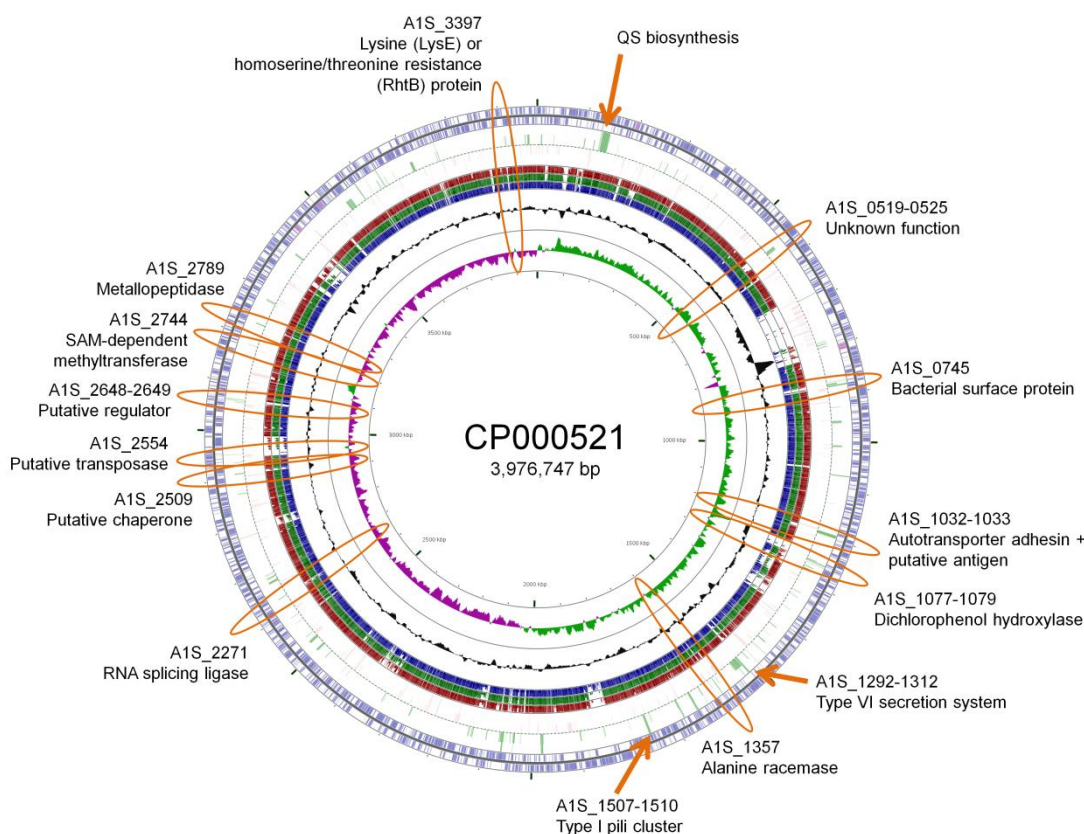


**Figure 5.12: Comparative analysis of the transcriptome results and genomic conservation**

The transcriptome results were incorporated into the circular representation of CP000521 (*A. baumannii* ATCC 17978). To identify potentially horizontally-acquired genomic regions, the Blastn analysis of CP000521, *A. baumannii* AYE, ACICU and WM99c were included. Genomic regions conserved between CP000521 (outer two rings in purple; sense out, antisense in) and AYE, ACICU and WM99c are represented in red, green and blue, respectively. The transcriptome data have been presented in the rings between the CP000521 and AYE genomes; genes up-regulated are represented by green bars and genes down-regulated in light-red bars. Half bars indicate genes more than 2-fold differentially expressed and full bars show genes differentially expressed by more than 4-fold. The two inner circles represent the GC-percentage and GC-skew, outer and inner, respectively. Various up-regulated genes or gene clusters, not fully conserved between CP000521 and the other genomes have been indicated by the orange circles, these highlighted locations were also investigated using Mauve (Section 2.7.2).

*Acinetobacter/E. coli* shuttle vector pWH1266 using *Bam*HI restriction sites, generating plasmid pWH0268 (Section 2.4.8; Table 2.3). The pWH0268 construct and empty vector (pWH1266) were introduced into freshly prepared competent *A. baumannii* 17978hm and B23 cells by electroporation (Section 2.4.13). The plasmids were maintained by selection with 100 µg/ml ampicillin. The introduction of the WT A1S\_0268 into strains 17978hm and B23 was confirmed by PCR using the A1S\_0268 specific oligonucleotides (Table 2.4). The PCR resulted in amplification of two products, representing WT A1S\_0268 and the larger insertionally inactivated 17978hm and B23 specific A1S\_0268 (data not shown). Motility assays (Section 2.3.4) showed that *A. baumannii* 17978hm (pWH0268) and B23 (pWH0268) cells were non-motile on semi-solid MH media, therefore showing an altered phenotype that was the same as WT cells (Table 5.3). Inhibition of pellicle formation and decreasing the cell surface hydrophobicity also occurred in both 17978hm (pWH0268) and B23 (pWH0268) (Table 5.3). Furthermore, investigation of transcription levels using qRT-PCR (Section 2.4.15) of the type VI secretion system (A1S\_1292) and a type I pili cluster (A1S\_1510) showed transcriptional repression by introduction of the WT A1S\_0268 ORF (pWH0268) (Table 5.3). These assays showed successful complementation of the altered phenotypes of strains 17978hm and B23, confirming that disruption of A1S\_0268 in these strains was responsible for the phenotypic changes. Moreover, analysis of the transcription levels also assisted in identification of potential regulatory targets of H-NS.

## **5.2.8 The effect of stress on motility and adherence**

### **5.2.8.1 The variant strain does not display differences in resistance**

The changes observed in strain 17978hm compared to ATCC 17978, such as increased hydrophobicity, may also affect other phenotypes, such as antimicrobial resistance. Therefore, resistance of WT and 17978hm cells to a range of antimicrobials was investigated by examining the MIC of these compounds. The MIC values were determined using a two-fold micro-dilution assay and a method using semi-solid agars (Section 2.3.2). The latter was used as motility on semi-solid MH media may affect resistance of the variant strain. The MIC to various structurally and functionally distinct compounds was examined, including ciprofloxacin, tetracycline, colistin, chlorhexidine and 2,2'-dipyridyl. These compounds were selected as they were also used in other stress assays described below. Susceptibility of WT and 17978hm cells to these compounds

**Table 5.3: Complementation of the *A. baumannii* ATCC 17978 A1S\_0268 mutant strains**

Strain	Motility <sup>a</sup>	Pellicle <sup>b</sup>	Hydrophobicity index (%)	Type VI secretion system <sup>c</sup>	Type I pili <sup>d</sup>
ATCC 17978	-	-	17		
17978hm	+	+	40	>1000	4
17978hm (pWH1266)	+	+	51	>1000	13
17978hm (pWH0268)	-	-	1		
B23 (pWH1266)	+	+	78	>1000	15
B23 (pWH0268)	-	-	1		

<sup>a</sup> Motility was investigated using MH media containing 0.25% agar.

<sup>b</sup> Pellicle formation was examined after static incubation for 24 hours in LB broth containing 100 mM NaCl.

<sup>c</sup> Expression of A1S\_1292, times-fold motile over non-motile cells.

<sup>d</sup> Expression of A1S\_1510, times-fold motile over non-motile cells.

was identical using either method (Table 5.4). However, cells of both strains were generally more resistant to higher concentrations of antimicrobials when tested using the agar-dilution method, as compared to the micro-dilution method (Table 5.4). Interestingly, various antimicrobial compounds, such as tetracycline and chlorhexidine, had an inhibitory effect on motility of strain 17978hm when performing the MIC assays on semi-solid MH media (Section 5.2.8.2).

#### 5.2.8.2 *Inhibition of motility as a result of environmental stress*

*A. baumannii* strain ATCC 17978 exhibits a motile phenotype on semi-solid LB media (Sections 3.2.5 and 4.2.2) (Mussi *et al.* 2010). LB media commonly includes 1% NaCl (~171 mM), however, variation of the salt concentration was found to have a major influence on the motility rate of *A. baumannii*. Therefore, motility was tested in different NaCl concentrations in LB, from 0 to 200 mM in 20 mM increments. *A. baumannii* ATCC 17978 showed the highest motility rates on LB medium supplemented with 100 mM NaCl, with similar results obtained when replacing NaCl with KCl (data not shown). Comparable results were obtained with strain 17978hm, however, the rate of motility was significantly higher compared to the WT strain under all conditions tested. Other environmental stress factors, such as blue-light (Mussi *et al.* 2010) or iron-limitation (Section 3.2.5), were previously shown to affect motility of strain ATCC 17978. Motility of strain 17978hm was also repressed under these stress conditions when investigating the MIC using semi-solid MH media (Section 5.2.8.1). Therefore, the effect of stress on motility was further investigated using various different stress conditions. Motility inhibition assays were performed by incubation with sub-inhibitory concentrations of the test compound, typically 50% of the MIC, in semi-solid MH media. The concentrations were decreased if initial growth at the inoculation site was affected. The following concentrations were used for further investigation of the effect of antimicrobial stress on motility; 0.128 µg/ml ciprofloxacin, 2 µg/ml tetracycline, 1 µg/ml colistin, 6 µg/ml chlorhexidine, 100 µg/ml ethidium and 0.2% SDS (Table 5.5). Motility was fully inhibited by sub-inhibitory concentrations of tetracycline and ethidium, and as described above, high-salt (supplementation with 100 mM NaCl) and low-iron conditions (200 µM 2,2'-dipyridyl). Phenotypic changes in motility were not observed when incubated with colistin or ciprofloxacin. Chlorhexidine resulted only in a minor reduction of surface translocation.

**Table 5.4: Antimicrobial MIC values of *A. baumannii* strain ATCC 17978 and 17978hm**

	Micro-dilution		Agar-dilution	
	ATCC 17978	17978hm	ATCC 17978	17978hm
<b>Ciprofloxacin</b> ( $\mu\text{g/ml}$ )	0.128	0.128	0.256	0.256
<b>Tetracycline</b> ( $\mu\text{g/ml}$ )	4	4	4	4
<b>Colistin</b> ( $\mu\text{g/ml}$ )	1	1	2	2
<b>Chlorhexidine</b> ( $\mu\text{g/ml}$ )	8	8	8	8
<b>2,2'-dipyridyl</b> ( $\mu\text{M}$ )	400	400	400	400

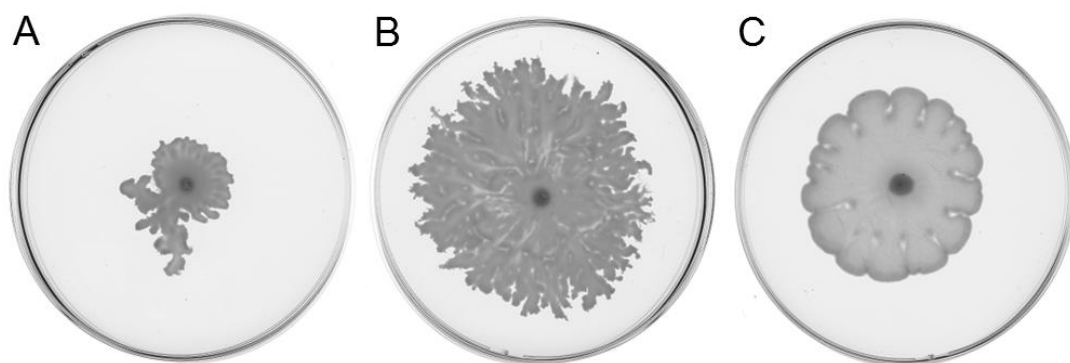


**Figure 5.13: Motility phenotypes of *A. baumannii* strain 17978hm under stress**

Incubation of strain 17978hm on MH containing 0.25% agar supplemented with 6  $\mu\text{g/ml}$  chlorhexidine and 100 mM NaCl (A), 1  $\mu\text{g/ml}$  colistin and 100 mM NaCl (B), or 2  $\mu\text{g/ml}$  tetracycline and 6  $\mu\text{g/ml}$  chlorhexidine (C). The motility plates were inoculated in the centre and incubated at 37°C for 24 hours (Section 2.3.4). Examples of an uninhibited motility phenotype and complete motility inhibition, achieved by supplementation with 2,2'-dipyridyl to the growth media, have been presented in Figure 3.7.

**Table 5.5: Motility of *A. baumannii* strain 17978hm under stress**

	Untreated <sup>a</sup>	Colistin (1 µg/ml)	Ciprofloxacin (0.128 µg/ml)	Chlorhexidine (6 µg/ml)
<b>Untreated</b>	+++	nd <sup>b</sup>	nd	nd
<b>Colistin</b> (1 µg/ml)	+++	nd	nd	nd
<b>Ciprofloxacin</b> (0.128 µg/ml)	+++	+++	nd	nd
<b>Chlorhexidine</b> (6 µg/ml)	++	+++	++	nd
<b>Tetracycline</b> (2 µg/ml)	-	-	-	++
<b>Ethidium</b> (100 µg/ml)	-	-	-	-
<b>2,2'-dipyridyl</b> (200 µM)	-	-	++	-
<b>SDS (0.2%)</b>	-	-	-	-
<b>NaCl</b> (100 mM)	-	+++	-	+

<sup>a</sup> - = no motility; + = motility zone  $\leq$  4 cm; ++ = motility zone  $\geq$  4 cm; +++ = complete coverage of the Petri dish.

<sup>b</sup> nd = not determined.

In various *A. baumannii* isolates, increasing salt concentrations were shown to result in higher resistance levels to colistin (Hood *et al.* 2010). Coincidentally, in this study it was determined that the motility phenotype of strain 17978hm under high-salt conditions could be restored when supplementing sub-inhibitory concentrations of colistin (Table 5.5; Figure 5.13). Therefore, motility was further investigated using combinations of different stress factors (Table 5.5). Restoration or partial restoration of the motility phenotypes was observed when using a combination of tetracycline and chlorhexidine, low-iron conditions and ciprofloxacin, and increased salinity in combination with chlorhexidine (Figure 5.13; Table 5.5). The size of the motility zone observed using different combinations was reproducible and the motility patterns appeared similar throughout multiple testings. Cells from the motile population of these restored phenotypes were subsequently tested for motility on the individual compounds, to ensure that no permanent changes were induced upon incubation with the combination of compounds (data not shown). A restored motility phenotype was not observed when investigating combinations of compounds that each independently resulted in inhibition of motility, such as tetracycline, ethidium, 2,2'-dipyridyl and SDS.

Since surface translocation is an energy consuming process, *A. baumannii* may not express its motility features when exposed to unfavourable conditions to conserve energy for survival. The restored motility phenotypes observed in the combination assays suggested that certain compounds, such as colistin and ciprofloxacin, promote motility of strain 17978hm.

### 5.2.8.3 *Stress on biofilm formation*

Multidrug resistant *A. baumannii* strains often possess a greater ability to form biofilms than their susceptible counterparts (Lee *et al.* 2008; Rajamohan *et al.* 2009; Rao *et al.* 2008). Biofilm induction upon incubation with sub-inhibitory concentrations of antimicrobials has also been shown. For example, an increase in biofilm formation in the presence of imipenem was observed in a pathogenic *A. baumannii* isolate (Nucleo *et al.* 2009). These findings are of major importance, as knowing whether certain antimicrobials may lead to increased or decreased levels of biofilm formation may prove advantageous for treatment of patients or in sanitation regimes. Therefore, biofilm formation of strains ATCC 17978 and 17978hm was investigated under different stress conditions (Figure 5.14). First, planktonic growth

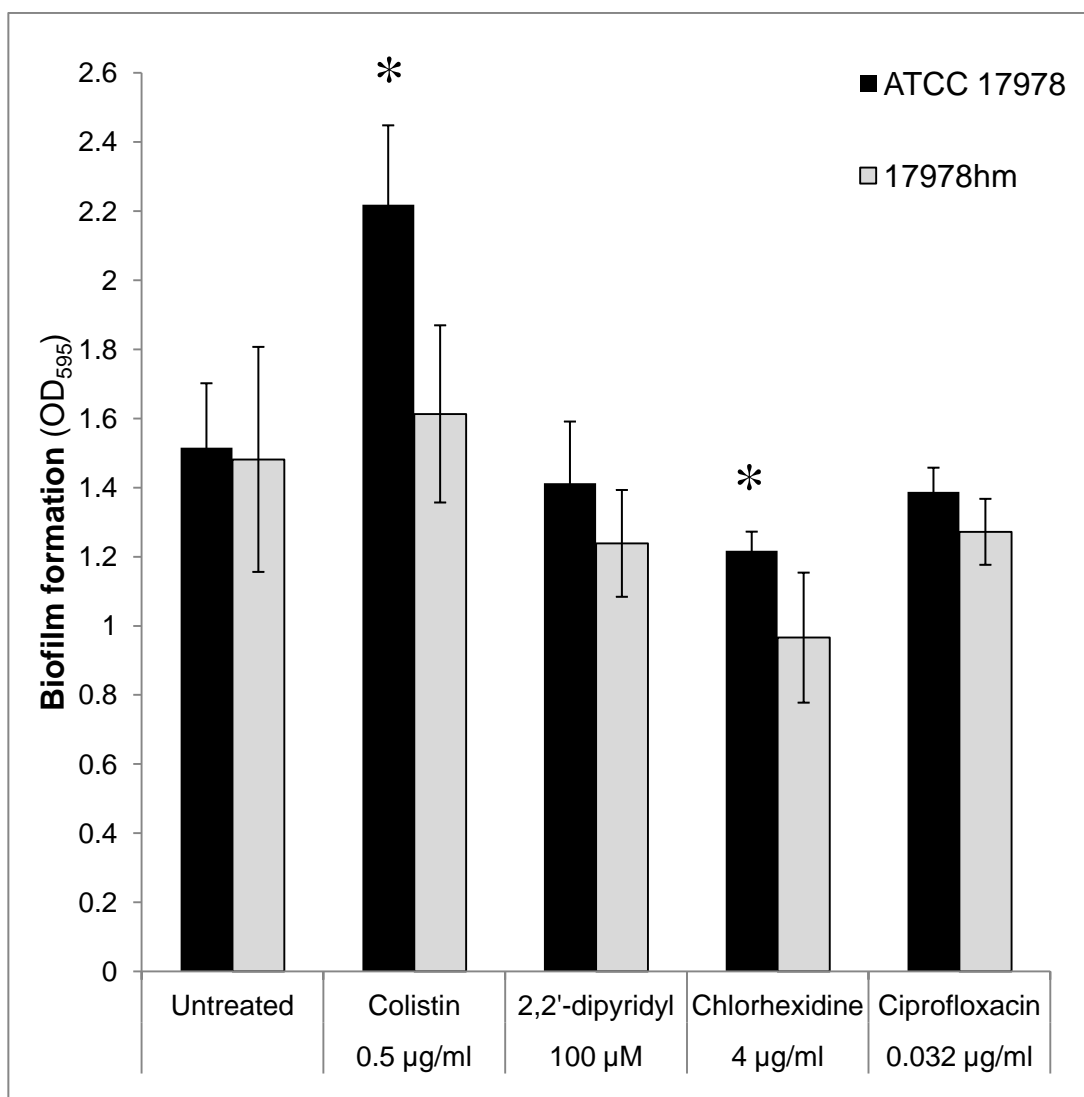


**Figure 5.14: Biofilm formation under stress conditions**

Biofilm production of strain ATCC 17978 (black) and strain 17978hm (grey) was examined using a static microtiter tray assay, adherent cells were stained using crystal violet and the biomass was determined by measuring the OD<sub>595</sub> (Section 2.3.3). Significant changes in biofilm formation upon exposure to stress was only observed in *A. baumannii* strain ATCC 17978; incubation with 0.5 µg/ml colistin resulted in significantly ( $p < 0.05$ ; student *t*-test) increased biofilm production and 4 µg/ml chlorhexidine resulted in a minor, but significant ( $p < 0.05$ ; student *t*-test), decreased level of biofilm formation by strain ATCC 17978 as compared to untreated ATCC 17978 cells. Incubation with 100 µM 2,2'-dipyridyl or 0.32 µg/ml ciprofloxacin had only minor effects on biofilm production by either strain. The data represent three experiments using at least triplicate wells. The error bars show the standard deviation.

was examined by measuring the OD<sub>600</sub> of the medium to ensure that growth under stress was not significantly different to that of untreated cells (Section 2.3.3). The concentrations of the compounds used to assess the effect of stress on biofilm formation by *A. baumannii* strains ATCC 17978 and 17978hm were slightly lower compared to those used for investigation of stress on the motility phenotype, as described above (Section 5.2.8.1). Here, the effect of 0.5 µg/ml colistin, 100 µM 2,2'-dipyridyl, 4 µg/ml chlorhexidine or 0.32 µg/ml ciprofloxacin on biofilm formation by strains ATCC 17978 and 17978hm was investigated (Section 2.3.3; Figure 5.14). Strain ATCC 17978 showed a significant increase in biofilm production when incubated with colistin. Other stress conditions resulted in minor changes, such as the slightly lower levels observed under chlorhexidine stress in both strain ATCC 17978 and 17978hm. Overall, unlike surface translocation, biofilm formation appeared more stable under stress.

#### **5.2.8.4 Pellicle formation is susceptible to environmental changes**

Pathogens such as *A. baumannii* are continuously exposed to antimicrobial stress in their environment. Investigating the effect of stress on pellicle formation may shed light on resistance and persistence strategies employed by *A. baumannii*. LB media containing 100 mM NaCl were used for investigation of environmental stress on pellicle formation by strain 17978hm (Sections 2.3.5 and 5.2.2.2). First, the effect of iron limitation on pellicle formation was investigated by supplementing 2,2'-dipyridyl to the growth media at varying concentrations. Whereas no differences were observed in biofilm formation (Section 5.2.8.3), iron-limitation by supplementation with 200 µM, 100 µM or 50 µM 2,2'-dipyridyl resulted in decreased pellicle biomass of strain 17978hm compared to the untreated control (Figure 5.15). Since oxygen is essential for pellicle formation (Section 5.2.2.2), impaired respiration due to lack of oxygen transport by iron or iron containing molecules may have resulted in the reduced pellicle biomass observed in the low-iron environment. Interestingly, pellicle formation was enhanced by supplementation with 0.128 µg/ml ciprofloxacin, the highest concentration at which planktonic growth remained unaffected. The almost 2-fold increase in pellicle formation observed with ciprofloxacin supplementation became less reproducible when lowering the concentration to 0.064, 0.032 or 0.016 µg/ml ciprofloxacin. Supplementation with 1 µg/ml colistin resulted in a lack of growth in some experiments and was therefore not considered suitable for further investigation (data

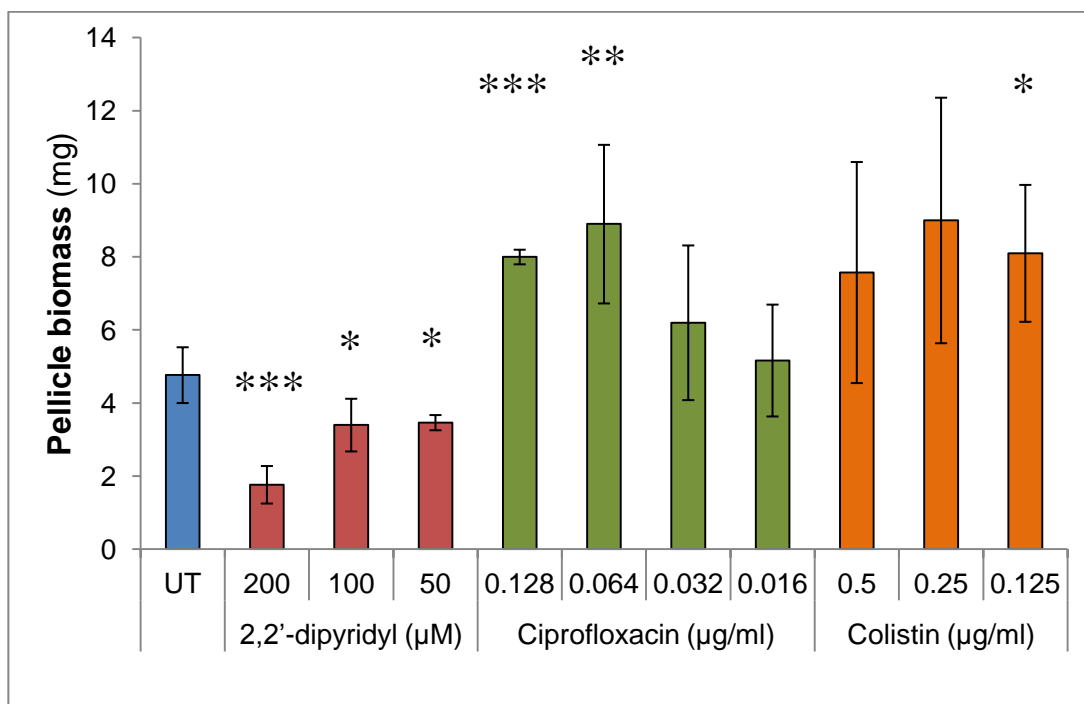


**Figure 5.15: Pellicle formation of *A. baumannii* strain 17978hm under stress conditions**

The pellicle biomass in milligrams (mg) was measured after incubation for 72 hours at 25°C in LB media containing 100 mM NaCl (blue) (Section 2.3.5). The effect of 2,2'-dipyridyl (red), ciprofloxacin (green) and colistin (orange) was investigated at varying concentrations. Statistical analyses were performed using a two-tailed student *t*-test and the results are represented by the asterisks;  $p < 0.05$  (\*),  $p < 0.005$  (\*\*) and  $p < 0.001$  (\*\*\*). The results represent an average of three independent experiments and the error bars display the standard deviation.

not shown). Lower concentrations of colistin, 0.5 µg/ml, 0.25 µg/ml and 0.125 µg/ml, showed an overall increase in pellicle formation. However, fluctuating results were obtained during three independent experiments under the same conditions. Generally, it appears that pellicle formation in strain 17978hm is susceptible to the stress conditions tested.

### 5.2.9 Transcriptional profiling of *A. baumannii* under stress conditions

Measuring mRNA levels under different stress conditions assists in examining the role of molecular mechanisms potentially involved in the virulence and persistence characteristics investigated in this study. The expression levels of a number of genes in strain 17978hm were investigated in cells grown on motility plates, defined as MH containing 0.25% agar (Sections 2.3.4 and 2.4.15). Investigation of transcription levels by qRT-PCR (Section 2.4.15) was also performed under conditions inhibitory to motility of strain 17978hm, such as low iron (200 µM 2,2'-dipyridyl) and high salt (100 mM NaCl). The effect of colistin (1 µg/ml) and ciprofloxacin (0.125 µg/ml) was also investigated; as shown above, both compounds did not affect the motility phenotype (Table 5.5).

As *Acinetobacter* species do not contain flagella, surface structures such as type IV pili are likely candidates for the mode of action behind surface translocation (Sections 1.2.4.3, 3.2.5 and 4.2.5). Transcriptomic analysis of motile and non-motile cells showed major transcriptional differences in QS-signal biosynthesis (A1S\_0109-0119) and the phenylacetic acid degradation pathway (A1S\_1335-1349) (Section 5.2.4.2). Therefore, transcription levels of representative genes of these molecular mechanisms and of the type IV pili were investigated under different stress conditions in semi-solid MH media (Table 5.6). The oligonucleotides used for qRT-PCR analysis (Section 2.4.15) of the genes described below have been provided in Table 2.4.

#### 5.2.9.1 Expression of *abaI* correlates with the motility phenotype

QS-signals may be involved in induction and promotion of motility in *A. baumannii*, as major up-regulation, approximately 30-fold, of *abaI* was observed in the motile *A. baumannii* 17978hm cells (Section 5.2.4.2). Hence, transcription levels of *abaI* were investigated under different stress conditions some of which are known to have an inhibitory effect on the motility of strain 17978hm (Section 5.2.8.2). Expression of *abaI* in strain 17978hm under highly saline (100 mM NaCl)

and iron-limiting conditions (200  $\mu$ M 2,2'-dipyridyl) was found to be at similarly low levels as those observed for non-motile ATCC 17978 cells on semi-solid MH media (Section 5.2.6; Table 5.6). Conversely, expression levels of more than 30-fold higher were observed when supplementation of the growth media with either 1  $\mu$ g/ml colistin or 0.125  $\mu$ g/ml ciprofloxacin, conditions which allow surface translocation to occur. Again, the difference observed in *abaI* expression levels indicated that QS-signals are produced only in motile cells, confirming the results obtained using semi-solid LB media (Section 5.2.6.1).

#### 5.2.9.2 Expression of type IV pili is highly responsive to iron limitation

Type IV pili, together with flagella, are the most well studied molecular mechanisms responsible for bacterial surface translocation (Section 1.2.4). The transcriptomic analysis performed in this study revealed no significant differential expression of type IV associated genes between cells of the motile and non-motile population (data not shown). This may indicate that either type IV pili are not essential for motility in *Acinetobacter* or motility is a multi-factorial process and type IV pili genes were in an 'on-state' in both populations, as *A. baumannii* strain ATCC 17978 does show motility on semi-solid LB media (Section 4.2.2). Down-regulation of type IV pili genes under iron-limitation was observed previously (Figure 3.6). Therefore, investigation of expression of the IV pili genes was extended using the different conditions described above (Section 5.2.9). Only genes or gene clusters encoding structural subunits of the type IV pili complex were investigated by qRT-PCR (Section 2.4.15) using the oligonucleotides described in Table 2.4.

Transcripts of a putative operon that included both *pilW* (A1S\_3168) and *pilE* (A1S\_3165) could not be detected by a qRT-PCR analysis using oligonucleotides specific to A1S\_3168 (data not shown). Transcription levels of these two genes under stress were for that reason not further investigated. Expression of *pilT* (A1S\_0897) and *pilM* (A1S\_3195) did not increase more than 2-fold under any of the conditions tested compared to those observed in untreated *A. baumannii* 17978hm cells, and were therefore not considered to be significantly differentially expressed (data not shown).

Expression levels of *pilB* (A1S\_0329) and the gene encoding the major fimbrial subunit, *pilA* (A1S\_3177), were heavily down-regulated under iron-limiting

**Table 5.6: Transcriptional responses of *A. baumannii* strain 17978hm under different stress conditions**

	ATCC 17978		17978hm			
	Untreated	Untreated	Colistin (1 µg/ml)	Cipro- floxacin (0.125 µg/ml)	2,2'- dipyridyl (200 µM)	NaCl (100 mM)
<b>Motile</b> <sup>a</sup>	-	+	+	+	-	-
<b>Quorum- sensing</b> ( <i>abaI</i> ) <sup>b,c</sup>	low	high	high	high	low	low
<b>Type IV pili</b> ( <i>pilA</i> ) <sup>b,d</sup>	high	high	high	high	low	high
<b>Type IV pili</b> ( <i>pilB</i> ) <sup>b,d</sup>	high	high	high	high	low	high
<b>Phenyl acetic acid degradation</b> (A1S_1336) <sup>b,e</sup>	high	low	low	low	low	high

<sup>a</sup> Examined on MH media containing 0.25% agar.

<sup>b</sup> Transcription levels normalised to *16s rDNA*.

<sup>c</sup> >30-fold difference between high and low.

<sup>d</sup> >1000-fold difference between high and low.

<sup>e</sup> >100-fold difference between high and low.

conditions as transcripts could not be detected when supplementing 200  $\mu\text{M}$  2,2'-dipyridyl to the growth medium (Table 5.6). Again, this points towards a possible involvement of type IV pili in *A. baumannii* motility. However, these results taken together with those obtained for non-motile cells in a highly saline environment, where no differential expression of the type IV pili genes was observed, support the possibility that motility is mediated by more than one molecular mechanism.

### 5.2.9.3 *The phenylacetic acid degradation pathway is highly up-regulated in a saline environment*

Although metabolism has not been directly associated with bacterial motility, transcription levels of *paaA* were further investigated under different environmental conditions as major transcriptional differences were observed in the microarray analysis (Section 5.2.4.2). *A. baumannii* ATCC 17978 cultures grown in MH broth under iron-limiting conditions showed minor down-regulation of the *paa* cluster (Appendix B). This complements the previous data revealing that Paa proteins are overexpressed under iron-rich conditions (Nwugo *et al.* 2011). However, *paaA* showed no transcriptional responses in 17978hm when cultured on iron-limiting semi-solid MH media (Table 5.6). This can be explained by the already low expression levels of *paaA* observed in 17978hm on semi-solid MH media, which may not significantly decrease under iron-limiting conditions.

Highly saline conditions are known to affect the catabolic activity of organisms (Abouseoud *et al.* 2010; Bazire *et al.* 2007; Darvishi *et al.* 2011). In this study, supplementation with 100 mM NaCl to semi-solid MH media resulted in major up-regulation of *paaA* in strain 17978hm (Table 5.6). The role of Paa proteins is in the benzoate degradation pathway (KEGG; [www.genome.jp](http://www.genome.jp)) and interestingly, the putative benzoate transporter protein (A1S\_1209) was previously shown to be up-regulated under highly saline conditions in *A. baumannii* (Hood *et al.* 2010). Other conditions, such as incubation with either colistin or ciprofloxacin did not result in significant up-regulation of *paaA*.

## 5.3 Conclusions

In this study, *A. baumannii* colonies showing a distinct morphology from its parental *A. baumannii* ATCC 17978 strain were isolated. Although initially isolated for its hyper-motile phenotype, the variant strain, called *A. baumannii* 17978hm, showed various other interesting characteristics. In general, strain 17978hm

possessed an enhanced adherence capacity compared to WT cells. The most striking differences were seen in pellicle formation and adherence to eukaryotic cells. Examination of the pellicle of strain 17978hm revealed that the intercellular interactions in this type of biofilm are unlikely to be facilitated by extracellular protein or DNA structures. Interestingly, strain 17978hm possessed more hydrophobic characteristics than its parental strain, which may be involved in the altered adherence and motility characteristics. The resistance profile of strain 17978hm was indifferent to that of WT cells.

Comparative transcriptomics was subsequently performed on WT ATCC 17978 and 17978hm cells grown on semi-solid MH media, on which only 17978hm exhibits a motile phenotype. Major transcriptional differences were seen in a type I pili cluster, a type VI secretion system, QS-biosynthesis, Lon protease and in various genes involved in metabolism, such as phenylacetic acid degradation. Expression levels of the aforementioned clusters were also investigated in WT and variant cells grown on semi-solid LB media on which both strains displayed a motile phenotype. The homoserine lactone synthase gene *abaI* was found to be expressed at similarly high levels in both strains, indicating that QS is directly linked to the motility state and was not a feature restricted to the hyper-motile variant.

The genetic differences between *A. baumannii* ATCC 17978 and 17978hm were investigated by whole genome sequencing. Numerous SNPs were identified in strain 17978hm, however, out of the 18 analysed, Sanger sequencing rebutted 17. The only confirmed SNP was not found in the independent hyper-motile strain, *A. baumannii* B23. This clearly eliminated this SNP as being solely responsible for the hyper-motile phenotype observed in strain 17978hm. The most striking difference in the genome comparison was observed in A1S\_0268, in which strain 17978hm possessed an insertion element, disrupting the A1S\_0268 ORF. Strain B23 possessed the same insertion sequence in A1S\_0268, although the exact target site within A1S\_0268 was different between the two strains. The *A. baumannii* ATCC 17978 genome contains two insertion elements with a high level of homology to the one identified in A1S\_0268 of *A. baumannii* 17978hm, indicating that this mobile genetic element containing A1S\_0628 may replicate at a relatively high rate. The WT A1S\_0268 sequence encodes a putative H-NS protein of the histone-like protein family. Generally, H-NS proteins function as transcriptional repressors and preferentially bind AT-rich regions. The genetic locus coding for the type VI secretion system,

which is considered to be horizontally-acquired and therefore AT-rich, has been shown to be a target for H-NS proteins in other bacteria, and this may explain the high levels of expression of this gene cluster in strain 17978hm. A WT copy of A1S\_0268 was introduced into *A. baumannii* strains 17978hm and B23 using the *Acinetobacter/E. coli* shuttle vector pWH1266. *A. baumannii* 17978hm and B23 complemented with WT A1S\_0268 lost their ability to migrate on semi-solid MH media, did not form pellicles and became more hydrophilic. Furthermore, transcription levels of the type VI secretion system and a type I pili cluster were repressed when a WT copy of A1S\_0268 was reintroduced into these mutant strains. This demonstrated that the altered phenotypes observed in *A. baumannii* strain 17978hm and B23 could be attributed to the inactivation of H-NS.

Investigation of motility, biofilm formation and pellicle formation under different environmental conditions revealed that 17978hm cells are highly responsive to stress. Motility was inhibited by low-iron and high-salt conditions, and by supplementation of ethidium, tetracycline and SDS. However, combinations of sub-inhibitory concentrations of colistin and high-salt concentrations, and ciprofloxacin and low-iron conditions, resulted in restored motility phenotypes. This indicated that certain antimicrobials, such as colistin and ciprofloxacin, may have a motility promoting effect in *A. baumannii*. Low-iron conditions negatively affected pellicle formation, this may potentially be due to oxygen deficiency resulting from reduced respiratory activity mediated by iron-containing molecules. As for motility, both colistin and ciprofloxacin had an enhancing effect and elevated the levels of pellicle biomass. The possible promotion of expression of virulence determinants upon exposure to sub-inhibitory concentrations of antibiotics raises concerns about conventional treatment regimes. Obtaining a comprehensive picture on responses of clonally and geographically distinct *A. baumannii* isolates to widely used antimicrobials may assist in optimising treatment and decontamination strategies.

The responses to stress were further investigated at a transcriptional level. Expression levels of *abaI* (QS-biosynthesis), *paaA* (phenylacetic acid degradation), and *pilA* and *pilB* (type IV pili) were investigated in 17978hm cells grown on semi-solid MH media supplemented with 2,2'-dipyridyl, NaCl, ciprofloxacin or colistin. As seen on semi-solid LB media described above, expression of *abaI* in 17978hm correlated with the cell's motility state. *abaI* was expressed at high levels when cells were motile (untreated, ciprofloxacin or colistin) and at low levels when non-motile

(low iron or high salt). Transcriptional profiling of genes encoding proteins of the type IV pili correlated with results obtained in the iron-limitation transcriptomic analysis (Section 3.2.5). Transcripts of *pilA* and *pilB* could not be detected when semi-solid MH media were supplemented with 2,2'-dipyridyl. Other stress factors did not result in differential expression levels of either *pilA* or *pilB*.

The *paa* cluster of strain 17978hm, which includes *paaA*, showed more than 100-fold up-regulation under saline conditions. Catabolic activity in bacteria can be enhanced by biosurfactant production, specifically when dealing with hydrophobic compounds (Prabhu and Phale 2003). Therefore, the low expression levels of the *paa* cluster in strain 17978hm on semi-solid MH media may be linked to its increased hydrophobic nature. Furthermore, salinity could affect biosurfactant production as described previously (Abouseoud *et al.* 2010; Darvishi *et al.* 2011). A function other than catabolism of phenylacetic acid has not been described for the *paa* cluster in *A. baumannii*. However, *B. cepacia paaA* and *paaE* null mutants exhibited lower levels of pathogenicity compared to WT cells in a *Caenorhabditis elegans* model system (Law *et al.* 2008). As such, it cannot be ruled out that alterations in expression of the *paa* cluster of *A. baumannii* could modulate virulence.

The data obtained in this study showed that the H-NS protein plays a pivotal role in regulation of various genes involved in persistence features of *A. baumannii*, such as motility and adherence. It was also shown that increased cell surface hydrophobicity in strain 17978hm may be involved in motility and adherence. The interplay between cell surface hydrophobicity and metabolism, potentially affected by high salinity, requires further investigation (Section 7.2.2). Transcriptional profiling showed that type IV pili are likely function in motility, as described previously (Section 3.2.5). The role of the highly expressed type I pili, an autotransporter adhesin and the type VI secretion system in strain 17978hm remains largely unknown. However, in *E. coli*, type VI secretion systems have been shown to affect expression of a type I pili cluster (de Pace *et al.* 2010). Therefore, up-regulation of the overexpressed type I pili cluster in strain 17978hm may be an indirect result of inactivation of H-NS by derepression of the type VI secretion system. Overall, the extensive characterisation of the differences between *A. baumannii* strain ATCC 17978 and 17978hm, using a wide variety of experimental approaches, assisted in identification of various novel mechanisms that are potentially involved in mediating persistence of *A. baumannii*.